INVESTIGATION OF NEAR-FIELD THMC COUPLED PROCESSES

Liange Zheng, Jonny Rutqvist, Jim Houseworth, Jim Davis, Ruth Tinnacher, Lianchong Li and Hui-Hai Liu

Lawrence Berkeley National Laboratory (LBNL)

July 29, 2011

TABLE OF CONTENTS

1. INTRODUCTION 4
2. Modeling Coupled THMC Processes with TOUGHREACT-FLAC 4
2.1 Overview of THMC Processes 4
2.2 Chemical-mechanical coupling..... 8
2.2.1 An elastic model for CM coupling. 10
2.2.2 The swelling pressure calculation based on diffuse double layer (DDL) theory and possible coupling with BBM..... 11
2.2.2.1 DDL theory 11
2.2.2.2 Swelling pressure calculation based on DDL theory 13
2.2.2.3 BBM and BExM for mechanical behaviour of expansive clay..... 14
2.2.2.4 Coupling BExM with DDL using TOUGHREACT-FLAC..... 15
2.3 Simulation test using TOUGHREACT-FLAC with linear elastic swelling model ... 16
2.3.1 Experimental data..... 16
2.3.2 TOUGHREACT-FLAC simulation results 17
2.4 Conclusions and Future work 22
3. Discrete Fracture Modeling for A Disturbed-Rock Zone in a Clay Repository 23
3.1 Disturbed-Rock Zone (DRZ) Fracturing 23
3.2 Potential Need for a Discrete Fracture Model to Represent the DRZ 25
3.3 Previous Discrete Fracture Network Modeling of the DRZ 26
3.4 Technical Developments and Issues for DFN Modeling..... 26
3.5 Future Directions 31
4. Experimental Study of Uranium Diffusion in Clay-Rich Environments and Bentonite . 31
4.1 Background and Research Objectives 31
4.2 Diffusion in Porous Media and Types of Diffusion Coefficients..... 33
4.2.1 Molecular Diffusion Coefficients..... 33
4.2.2 Effective Diffusion Coefficients..... 34
4.2.3 Apparent Diffusion Coefficients 35
4.2.4 Contaminant Transport Driven by Diffusion 36
4.2.5 Proposed Approach: De-Coupling of Diffusion and Metal-Mineral Interactions 38
4.3 Typical Experimental Setups Used in Diffusion Studies..... 38
4.3.1 Steady-State Methods..... 38
4.3.2 Transient Methods..... 40
4.3.2.1 Column Methods..... 40
4.3.2.2 Half-Cell Methods..... 41
4.3.2.3 Reservoir Methods 42
4.3.3 Strategies for Sample Analysis and Characterization 44
4.3.4 Quality Assurance and Control 46
4.4 Summary of Current Knowledge of Uranium Diffusion..... 46
4.4.1 Uranium(VI) Aqueous Speciation..... 46
4.4.2 Clay-Rich Soils and Sediments 49

4.4.3 Claystone Formations 50
4.4.4 Bentonite 51
4.5 Research Needs and Plans 51
4.5.1 Research Plans 52
5. Summary 53
References 55

1. INTRODUCTION

Geological repositories for disposal of high-level nuclear waste generally rely on a multibarrier system to isolate radioactive wastes from the biosphere. This multibarrier system typically consists of a natural barrier system (NBS), including repository host rock and its surrounding subsurface environment, and an engineered barrier system (EBS). The EBS includes the man-made, engineered materials placed within a repository, including the waste form, waste canisters, buffer materials, backfill and seals (OECD, 2003). Both NBS and EBS play significant roles in the containment and long-term retardation of radionuclide release.

The EBS and near-field NBS are involved in complex thermal, hydrogeological, mechanical and chemical processes, such as heat release resulting from radionuclide decay, multiphase flow (including gas release resulting from canister corrosion), swelling of buffer materials, radionuclide diffusive transport, waste dissolution, and chemical reactions. All these processes are related to each other. An in-depth understanding of these coupled processes is critical for any performance assessment (PA) for EBS, NBS, and the entire repository.

This report documents the progress that LBNL has made in the "Repository Science-THCM Near Field" work package, including work activities: (1) development of fully coupled THCM modeling capability, (2) discrete fracture modeling of a clay-repository disturbed rock zone, and (3) experimental study of diffusion in EBS buffer (bentonite). Progress in developing international collaborations in the THCM area is documented in a separate report entitled "*Disposal R&D in Used Fuel Disposition Campaign: A Discussion of Opportunities for Active International Collaborations*" (Birkholzer, 2011).

These research activities address key Features, Events and Processes (FEPs), which have been ranked in importance from medium to high, as listed in Tables 7 and 8 of the *Used Fuel Disposition Campaign Disposal Research and Development Roadmap* (FCR&D-USED-2011-000065 REV0) (Nutt, 2011). Specifically, they address FEP 2.2.01.01, Excavation Disturbed Zone (EDZ); FEP 2.2.05.01,02,03, Flow and Transport Pathways; and FEPs 2.2.08.01,03,04,05,06 and 2.1.08.03, 07, 08, Hydrologic Processes; FEPs 2.2.07.01 and 2.1.07.02, 03, 04, 09, Mechanical Processes; FEPs 2.2.09.53,55,57 and 2.1.09.52, 53, 54 Chemical Processes—Transport, FEPs 2.1.04.01, Buffer/Backfill; and FEP 2.1.11.04, Thermal Processes.

2. MODELING COUPLED THMC PROCESSES WITH TOUGHREACT-FLAC

2.1 Overview of THMC Processes

The long-term chemical and mechanical stability of protective bentonite buffers and tunnel backfill, as well as the stability of the surrounding host rock, are key issues for the long-term performance of backfilled, multiple-barrier nuclear waste repositories. Such long-term

chemical and mechanical phenomena are impacted by temperature and hydraulics and as well as coupled thermal-hydrological-mechanical-chemical (THMC) coupled processes (Figure 2-1). For example, in the Swedish program for nuclear waste disposal, a number of so-called safety-function indicator criteria are defined, and many of those are related to the long-term stability of buffer and backfill. A certain swelling pressure should be maintain to keep the buffer homogenous, to prevent canister sinking, to prevent adverse effects from external rock-shear movement, to limit colloid transport, and to prevent the buffer from being a preferred pathway for radionuclide transport (Rutqvist and Tsang 2008). In soil mechanics, clay swelling or drying shrinkage are traditionally modeled in a simplified fashion, usually assuming that swelling strain is a function of moisture content (Rutqvist and Tsang 2008). Such a simplified approach may be justified if the chemical composition of the pore water were to remain constant over the long term. However, in reality, the long-term stability of the buffer is governed by coupled THMC processes— responding to increase in temperature or intrusion of saltwater that may lead to a loss of swelling pressure, and consequently a loss of the buffer's protective functions.

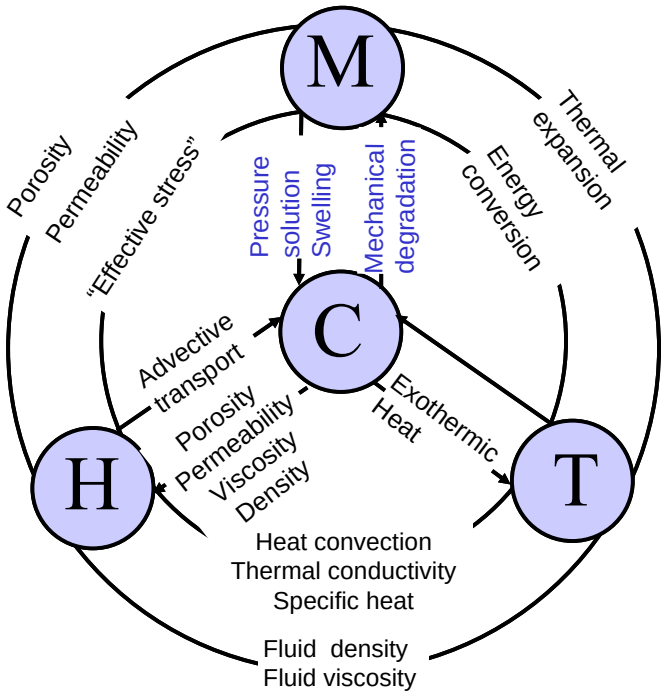

Figure 2-1. THMC processes that take place on a small scale (clay microstructure, rock grain contacts, microfractures), but dictate large-scale behavior of geological media.

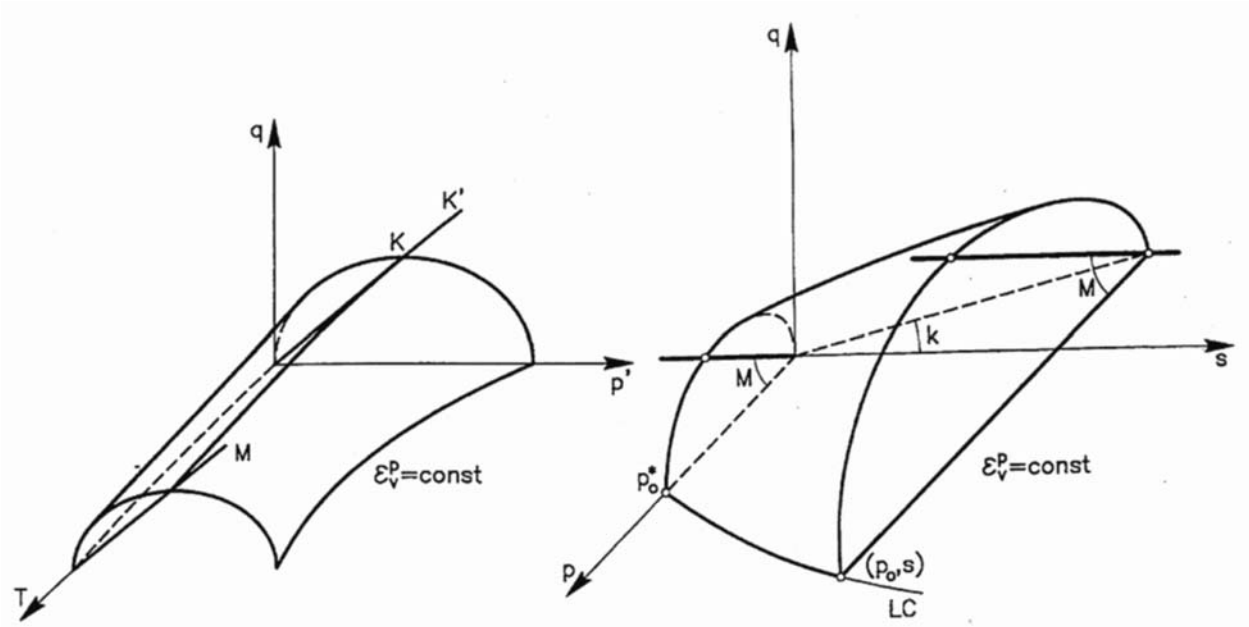

Figure 2-2. Three-dimensional representation of the yield surface in the thermo-elasto-plastic BBM (Rutqvist et al. 2011).

In 2009-2010, LBNL implemented the Barcelona Basic Model (BBM) into the coupled multiphase fluid flow and geomechanical simulator TOUGH-FLAC for rigorous modeling of thermo-elasto-plastic behavior of unsaturated soils (Rutqvist et al. 2011). The BBM can capture much of the typical mechanical behavior of unsaturated soil, including wetting-induced swelling or collapse strains, as well as increases in strength and stiffness with drying (Figure 2-2). The BBM is the most widely accepted model and is currently used by European and Japanese nuclear waste organizations for geomechanical modeling of clay-buffer systems. The implementation of the BBM into TOUGH-FLAC was verified and tested against several published numerical model simulations and laboratory experiments involving coupled thermal-hydrological-mechanical (THM) behavior of unsaturated soils. TOUGH-FLAC simulator with the BBM is now fully operational and ready to be applied to problems associated with nuclear waste disposal involving bentonite-backfilled tunnels, and other scientific and engineering problems related to the mechanical behavior of unsaturated soils (Rutqvist et al. 2011).

As a result of successful implementation and demonstration of the TOUGH-FLAC simulator combined with the BBM, the approach taken here is to extend the current model for a more complete representation of expansive clays, including the so-called double-structure behavior. In such an approach, a given material consists of two structural levels: a microstructure within which interactions occur at a particle level, and a macrostructure that accounts for the overall fabric arrangement of the material (comprised of aggregates and macropores) (Figure 2-3) (Gens et al. 2006; Sánchez et al. 2005; Gens and Alonso 1992). The double-structure approach is especially useful when trying to incorporate the effects of chemical variables on the mechanical behavior of bentonite buffer containing expansive clays. Because of its large proportion of active clay minerals, bentonite buffer are

especially susceptible to changes in the geochemical environment. Coupled geochemical-geomechanical processes that might affect the long-term stability and performance of the buffer include (Push, 2006; Villar et al. 2006):

1) The swelling and swelling pressure that can be achieved generally decreases with the saline content of pore water
2) Conversion of smectite to nonexpansive mineral forms ("illitization")
3) Cementation by precipitation of silica.

These are coupled THMC processes not necessarily confined within the buffer, but in the case of clay-rock repositories, the swelling, illitization, and cementation of the clay-based host rock itself may also have important implications for long-term repository performance.

The aforementioned coupled THMC processes can be simulated by numerical modeling, (e.g., by a coupling of LBNL's TOUGHREACT code to a geomechanical code such as $FLAC^{3D}$). In the case of a bentonite buffer, the BBM model, with its double structure clay model, can provide the necessary link for such a coupling. In such a case, the microstructure may be modeled by an physiochemical model (e.g., diffuse double layer theory), and while the resulting strains are assumed to be largely reversible, they may cause irreversible strains in the macrostructure. In a TOUGHREACT-FLAC3D coupled simulation, the chemically induced microstructural swelling strain calculated in TOUGHREACT can be transferred to FLAC3D, where it would enter the mechanical macrostructural calculation.

Another class of THMC phenomena, related to rock-strength degradation and creep in underground excavations, may impact the long-term performance of a nuclear waste repository. Such phenomena are usually modeled as a purely mechanical response with a time-dependent change in rock strength based on a logarithmic extrapolation in time from results of relatively short-term mechanical creep experiments. However, creep and long-term strength degradation is primarily a result of stress corrosion—that is, it is a result of chemical-mechanical coupling. Thus, a simple logarithmic extrapolation of its time-dependent behavior can be justified if the chemical composition of the pore water remains constant over the long term. This kind of phenomena can also be modeled mechanistically at the microstructural level, e.g., microfractures that grow as a result of chemically induced subcritical crack growth.

Currently, our work is focused on model development of linked TOUGHREACT-FLAC for coupled THMC modeling applied to swelling phenomena in bentonite and backfill. The ultimate goal in this context is to develop the chemo-mechanical link through the diffuse double layer theory (DDL) and BBM with the double structure model, using TOUGHREACT-FLAC3D. Variations in such an approach may also be applied to clay host rock. In this status report, we summarize our approach as well as current progress and initial modeling results that demonstrate the approach when applied to a swelling experiment on bentonite. Currently, we have linked TOUGHREACT and FLAC3D for running coupled THMC simulations, and we have tested and demonstrated the application of TOUGHREACT-FLAC3D to swelling phenomena in bentonite, using a simple

hydration swelling model extended to include chemically induced swelling. The next step will be to then develop and test the proposed THMC swelling model, based on DDL-BBM coupling, against rigorous TOUGHREACT-FLAC modeling applications.

2.2 Chemical-mechanical coupling

Geochemical changes in EBS bentonite or a surrounding clay formation can change the swelling properties therein. As mentioned above, the swelling of bentonite used as a protective buffer around a waste canister has important implications for long-term waste isolation (Rutqvist and Tsang 2008). Many laboratory experiments as well as full-scale field experiments have been conducted to study the geomechanical behavior of such bentonite-based buffers, including the study of swelling properties under various temperature and chemical conditions. For repositories located in clay host rock, such as shale, the swelling of the host rock itself may also have important implications for repository performance. For example, Wakim et al. (2009) conducted a series of free swelling tests using different types or concentrations of solution, and found that the more concentrated solution led to less swelling of shale, and that the type of solution (such as CaCl vs NaCl) also affects swelling. Thury (2002) reported that in contact with water, decompressed Opalinus Clay swells; the swelling varies when the swelling tests are carried out with various water types (deionized water, low mineralized water, synthetic pore water, and KCl solution). The maximum measured swelling heave (obtained with deionized water) perpendicular to bedding is 9%, and is up to 10 times greater than that parallel to bedding. More highly mineralized waters result in smaller (2% only) swelling heaves. Kamei et al. (2005) and Cuadros (2006) indicated that illitization, the transformation from smectites to illites, is usually part of the diagenesis process of clay formation—and that illitization apparently changes the swelling properties of a clay formation. Several simulations by Montes-H et al. (2005) have shown that Na/Ca-montmorillonite-to-Ca-montmorillonite conversion, caused by cation exchange in the interface, was a significant chemical transformation that could change swelling properties. The neo-formation of chlorites (nonswelling clays) (Montes-H et al., 2005) was also observed as a potential chemical transformation that could lower the swelling properties of clay rock.

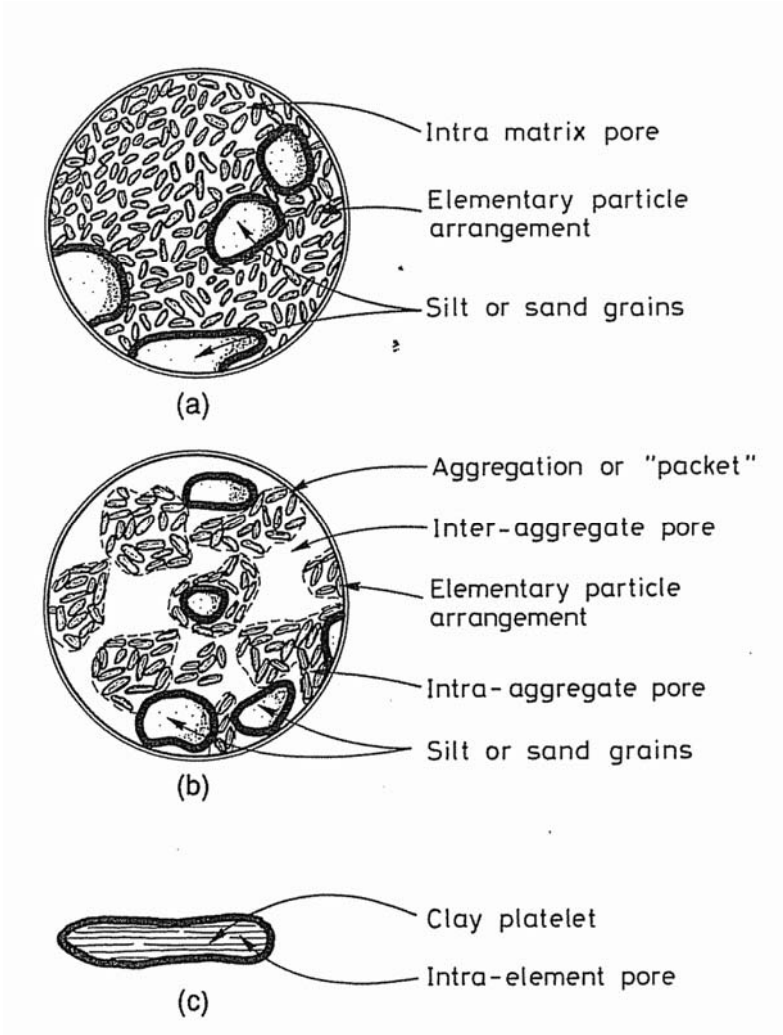

Figure 2-3. Fabric types in clay considered in a double structure model of expansive clay. (Gens and Alonso 1992)

Although geochemically induced swelling-property changes have been demonstrated experimentally and understood qualitatively, the mathematical link between chemical change and swelling pressure (or strain) has not yet been well established. For instance, some simulators have the capability of simulating THMC processes simultaneously, but the mechanical-chemical (MC) coupling is largely missing (Guimarães et al. 2007; Zheng et al. 2010). In this study, we linked the reactive transport code TOUGHREACT Version 2 (Xu et al. 2011) with the geomechanical code FLAC3D, enabling us to calculate THMC processes simultaneously. For initial testing and demonstration of the THMC simulator, we applied two types of MC coupling: (1) a simple linear elastic swelling model, and (2) a swelling model based on the Gouy-Chapman diffuse double layer (DDL) theory, as described in the following subsections.

2.2.1 An elastic model for CM coupling.

Laredj et al. (2010) extended a nonlinear elastic model (Thomas and He 1995) by adding a chemical concentration term. It is assumed that the increment of total strain can be given by the sum of the strain increments caused by the changes in net mean stress, suction, and chemical solute concentration:

$$d\varepsilon = d\varepsilon_p + d\varepsilon_s + d\varepsilon_n \tag{2-1}$$

where the subscripts p, s and n refers to net mean stress, suction and chemical solute concentrations. The stress-strain relationship can be expressed as:

$$\begin{aligned} d\sigma &= D(d\varepsilon - d\varepsilon_s - d\varepsilon_n) \\ &= D(d\varepsilon - A_s ds - A_n dn) \end{aligned} \tag{2-2}$$

with

$$d\varepsilon_s = A_s ds \tag{2-3}$$

$$d\varepsilon_n = A_n dn \tag{2-4}$$

where D is the elastic matrix, and A_s and A_n are constants, n is the ion concentration of the porewater. The strain resulting from chemical solute concentration changes was taken as the difference between the suction-related strain and the experimentally observed strain. Laredj et al. (2010) obtained the relationship between chemical concentration variation and the corresponding strain and proposed the following expression for A_n:

$$A_n = -\frac{(5.312 \ln c - 23.569)}{\sqrt{n}} - \frac{7.252 \times 10^{-4}}{n^2} \tag{2-5}$$

Rutqvist et al. (2011) included a linear elastic swelling model using a swelling strain that is linearly proportional to the saturation degree:

$$d\sigma = 3K\beta_{sw} ds_l \tag{2-6}$$

where K is the bulk modulus and β_{sw} is a moisture swelling coefficient and s_l is the saturation.

In this report, to consider the swelling resulting from both moisture and chemical concentration change, we include the strain resulting from chemical concentration change into Equation (2-6) as:

$$d\sigma = 3K\beta_{sw} ds_l + A_n dn \tag{2-7}$$

2.2.2 The swelling pressure calculation based on diffuse double layer (DDL) theory and possible coupling with BBM

2.2.2.1 DDL theory

While DDL theory has been applied extensively to assess the compressibility (or swelling) of initially saturated clays (Bolt 1956; van Olphen 1977; Sridharan and Jayadeva 1982; Madsen and Muller-vonmoss 1985; Mitchell and Soga 2005), researchers have also applied the theory to calculate the swelling pressure of unsaturated compacted bentonite used in EBS (Komine and Ogata 1996; 2003; Tripathy et al., 2004; Schanz and Tripathy, 2009). Tripathy et al. (2004) and Schanz and Tripathy (2009) present an extensive review of the application of the DDL theory to compacted bentonite and discussed some of its limitations. Tripathy (2004) applied the DDL theory to calculate the swelling pressure of FEBEX bentonite (ENRESA 2000) and tested it against the measured swelling pressure.

According to the DDL theory (Bolt 1956), the swelling pressure is the difference between the osmotic pressure in the central plane between two clay plates and the osmotic pressure in the equilibrium solution. In other words, the swelling pressure is the pressure required to keep the clay-water system at the required void ratio, when it is allowed to adsorb water or electrolyte (Tripathy et al. 2004). Bolt (1956) and van Olphen (1977) presented a method for calculating the swelling pressure in a clay–water electrolyte system. Sridharan and Jayadeva (1982) improved on Bolt (1956) and van Olphen (1977) and presented the diffuse double layer theory in a lucid form that could be readily used for understanding the engineering behavior of clays. The equations used by Sridharan and Jayadeva (1982) to determine swelling pressure are given in Equations (2-8) to (2-12):

$$e = G\gamma_w Sd \tag{2-8}$$

where e is the void ratio, G is the specific gravity of soil solids, γ_w is the unit weight of water, S is the specific surface area of soil (m^2/g swelling clay), and d is half the distance between parallel clay platelets.

$$\int_z^u \frac{1}{\sqrt{(2\cosh y - 2\cosh u)}} dy = \int_0^d d\xi = -Kd \tag{2-9}$$

where u is the nondimensional midplane potential, z is the nondimensional potential at the clay surface, y is the nondimensional potential at distance x from the clay surface, and ξ is the distance function (= Kx). K (1/m) is the double layer parameter:

$$K = \sqrt{\left(\frac{n(e')^2 v^2}{2\varepsilon kT}\right)} \tag{2-10}$$

where e' is the elementary electric charge (= 1.6×10^{-19} C), k is Boltzmann's constant (1.3806×10^{-23} j/K), n is the molar concentration of ions in pore fluid (molal), v is the valency of the interlayer cation, T is the absolute temperature, ε is the dielectric constant of the pore fluid, given by $\varepsilon = \varepsilon_0 D$, in which ε_0 is the permittivity of the vacuum (8.8542×10^{-12} $C^2J^{-1}m^{-1}$), and D is the ratio of the electrostatic capacity of condenser plates separated by the given material to that of the same condenser with a vacuum between the plates (Mitchell and Soga 2005)

$$\begin{aligned} -\left(\frac{dy}{d\xi}\right)_{x=0} &= \sqrt{(2\cosh z - 2\cosh u)} \\ &= \Gamma\sqrt{\left(\frac{1}{2\varepsilon nkT}\right)} \qquad at \quad x = 0, y = z \\ &= \left(\frac{B}{S}\right)\sqrt{\left(\frac{1}{2\varepsilon nkT}\right)} \end{aligned} \tag{2-11}$$

where Γ is the surface-charge density (base exchange capacity per specific surface), and B is the base exchange capacity of the clay (meq/100 g solid).

$$p = 2nkT(\cosh u - 1) \tag{2-12}$$

where p is the osmotic pressure or swelling pressure (Pa). For any given pore-fluid medium, determination of the swelling pressure using Langmuir's equation (i.e., Equation (2-13)) requires the nondimensional midplane potential function, u.

Determination of u is an indirect and time-consuming process. A relationship between u and the nondimensional distance function, Kd, must be established to determine u for any given value of Kd and vice versa. Equations (2-8)–(2-12) are used for this purpose. The details of the procedure for obtaining the u-Kd relation are given in Tripathy (2004).

Note that Equation (2-8) is valid for a pure swelling clay mineral, assuming that the clay platelets within a clay grain are packed in parallel. However, EBS bentonite is usually composed of some nonswelling minerals, and moreover the host clay rock sometimes contains only a small percentage of swelling clay. Equation (2-8) is therefore modified when applied to a mixture of nonswelling and swelling minerals (Wang et al. 2011):

$$e = G\gamma_w S f^s d(1 + f^d) \quad (2\text{-}13)$$

where f^s is the mass fraction of the swelling clay in the mixture, f^d is the ratio of the half distance between two nonswelling mineral platelets to *d,* the half distance between parallel clay platelets. In a broader sense, f^d represents the ratio of pore space associated with nonswelling minerals to that associated with swelling minerals. Typically, a nonswelling clay mineral, such as kaolinite or illite, has a the basal spacing (d(001)) of around 10 A, whereas a swelling clay (smectite) that undergoes osmotic swelling has the d(001) value of 20 to 40 A (Onikata et al. 1999). f^d therefore ranges from 0.25 to 0.5.

2.2.2.2 Swelling pressure calculation based on DDL theory

The DDL theory has been applied to assess the compressibility (or swelling) of initially saturated clays (Bolt 1956; van Olphen 1977; Sridharan and Jayadeva 1982; Madsen and Muller-vonmoss 1985; Mitchell and Soga 2005). When applying DDL theory to an unsaturated compacted bentonite system, some factors may affect DDL applicability (Schanz and Tripathy 2009), including (1) poorly developed or partially developed diffuse double layers, (2) reduced specific surface area because of the formation of clay particles, (3) surface and ion hydration at close platelet spacing, (4) existence of electrical attractive forces, and (5) the presence of various types of exchangeable cations. Because of these factors, the DDL theory in general does not work well for calculating the swelling pressure of compacted bentonite (Tripathy et al. 2004; Schanz and Tripathy 2009), especially when the dry density of compacted bentonite is higher than 1.6 Mg/m^3. Figure 4 shows the measured swelling pressure for FEBEX bentonite (ENRESA 2000) and the calculated values. In applying DDL theory to calculate the swelling pressure, the key is to establish the *u-Kd* relationship. As shown in Figure 2-4, the calculated swelling pressure using the *u-Kd* relationship obtained from Equations (8)–(13) deviates from the measured values incrementally as the dry density increases. The *u-Kd* relationship can also be back-calculated from the experimental data (called the experimental *u-Kd* relationship in Figure 2-4), which leads to better measured data, as expected. The *u-Kd* relationship is taken from Tripathy et al. (2004), with $u = -7.72 - 10.427 \log_{10} Kd$.

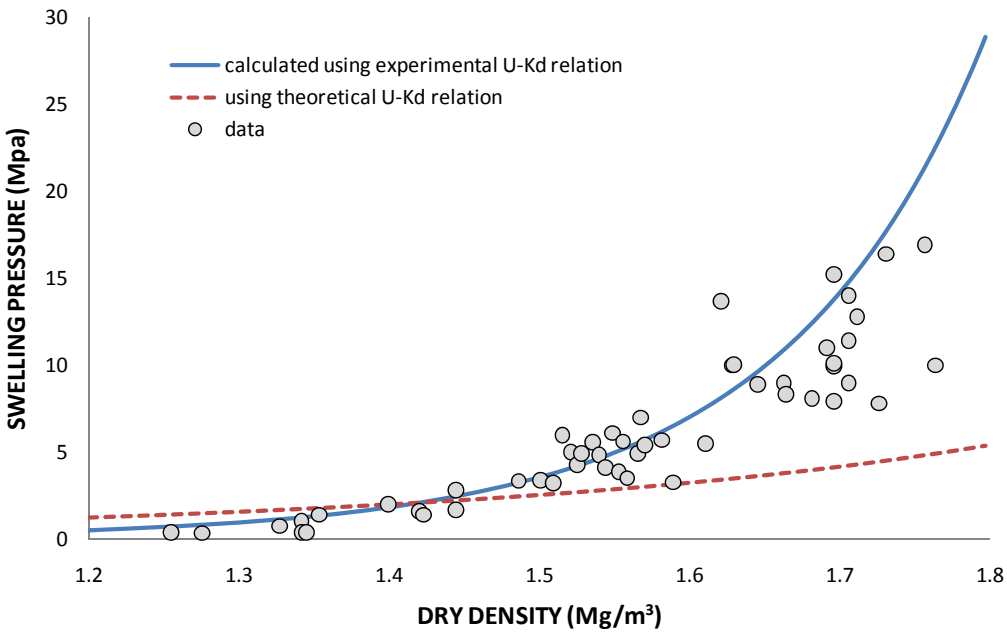

Figure 2-4. Comparison of measured (ENRESA 2000) and calculated swelling pressure for FEBEX bentonite.

2.2.2.3 BBM and BExM for mechanical behaviour of expansive clay

Currently, the existing BBM implementation is being extended to the expansive clay double structure behavior within the UFD EBS work package. This involves an extension of the elasto-plastic formulation to consider the mechanical behavior of the two structural levels and their interaction. We have identified an approach and suitable mathematical formulation (Alonso et al. 1999), equivalent to the Barcelona Expansive Model (BExM). The formulation is being implemented in C++ routines within the User Defined Model framework of the FLAC3D simulator. Once implemented, it will be verified and tested against published data. For example, Alonso et al. (1999) present such experimental data and numerical tests. Using this model, we will be able to properly model both micro- and macrostructure deformations and their interactions (Figure 2-5). .

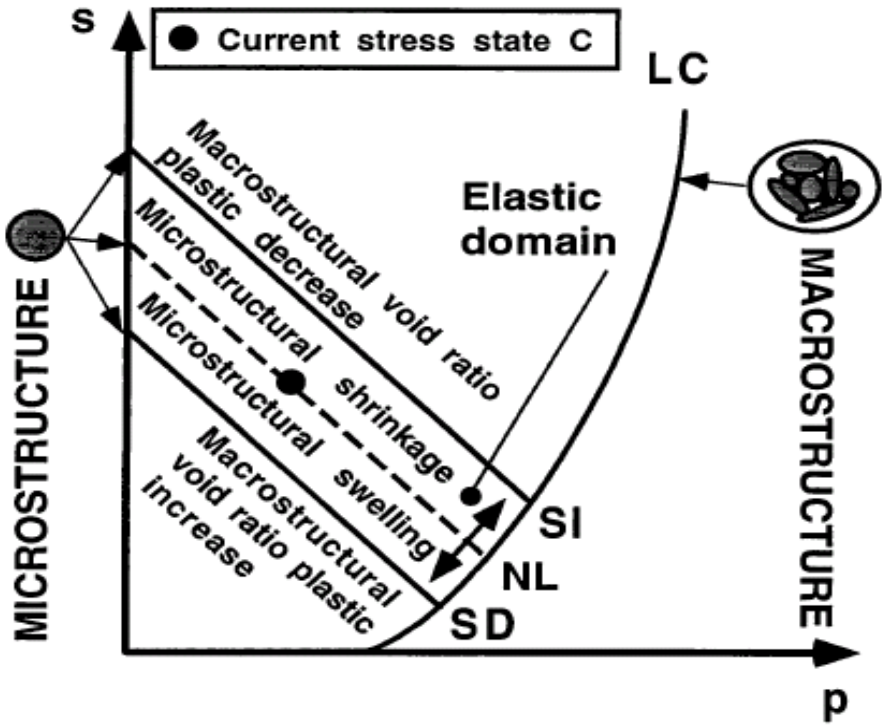

Figure 2-5. Showing microstructural and macrostructural elastoplastic responses in a double-structure model equivalent to the Barcelona Expansive Model.

2.2.2.4 Coupling BExM with DDL using TOUGHREACT-FLAC

As mentioned, the BBM model, which incorporates a double-structure clay model (BExM), can provide the necessary link for such a coupling. The microstructural swelling in the BExM is essentially the swelling in the interlayer space where a diffuse double layer exists. Considering that the microstructural strain can be linked to the porosity index (Equation (2-8)) or the change of thickness of diffuse double layers (or the distance between parallel clay platelets), the DDL theory, which establishes the relationship between swelling pressure and thickness of diffuse double layers (Section 2.2.2.1) allows us to establish the relationship between swelling stress and microstructural strain. Thus, a chemically induced swelling strain calculated by TOUGHREACT can be transferred to FLAC3D mechanical modeling, as a microstructural strain, which in the BExM is assumed to be largely reversible, but may cause irreversible strains in the macrostructure. The actual geomechanical response of such a swelling strain depends on the mechanical boundary conditions of the clay sample. For example, in a laboratory test for swelling stress, the sample would be fully constrained and the maximum swelling stress would be developed. If the sample is free to expand, the free swelling strain can be determined directly from the volumetric change of the sample.

2.3 Simulation test using TOUGHREACT-FLAC with linear elastic swelling model

We have linked TOUGHREACT and FLAC3D to provide the necessary numerical framework for coupled THMC simulations. In this section, we describe the application of TOUGHREACT-FLAC3D to swelling phenomena in bentonite, using a simple linear elastic swelling model extended to include an additional component of chemically induced swelling. Specifically, we simulate swelling tests conducted on FEBEX bentonite.

2.3.1 Experimental data

Swelling pressure tests were conducted on fully confined samples wetted to full saturation. In this case, samples were the bentonite material used in the FEBEX *in situ* experiment as part of the international collaborative project DECOVALEX (Alonso et al. 2005). The swelling pressure tests were performed using conventional odometers on samples saturated with distilled water. A regression curve was developed for the swelling pressure of the FEBEX bentonite, as shown in Figure Y (solid line), and as expressed by the equation

$$P_s = \exp\,(6.77\ \rho_d - 9.07)$$

where P_s is the swelling pressure in MPa and ρ_d is the dry density in g/cm^3. The deviation of the experimental values with respect to this fitting may be as high as 25%. The dispersion observed in the values is larger for higher dry densities, probably because of technical limitations, since the load capacity of the odometers is nearly exceeded by the swelling pressure.

The swelling-pressure values and the regression curve for the bentonite S-2 are also shown in Figure 6. The differences between the swelling pressures of the S-2 and the FEBEX bentonite may be considered negligible for practical purposes. For a dry density of 1.6 g/cm^3 and 65% initial saturation, a swelling pressure of about 5 to 6 MPa developed at full saturation (Alonso et al. 2005); this is the case modeled in this study.

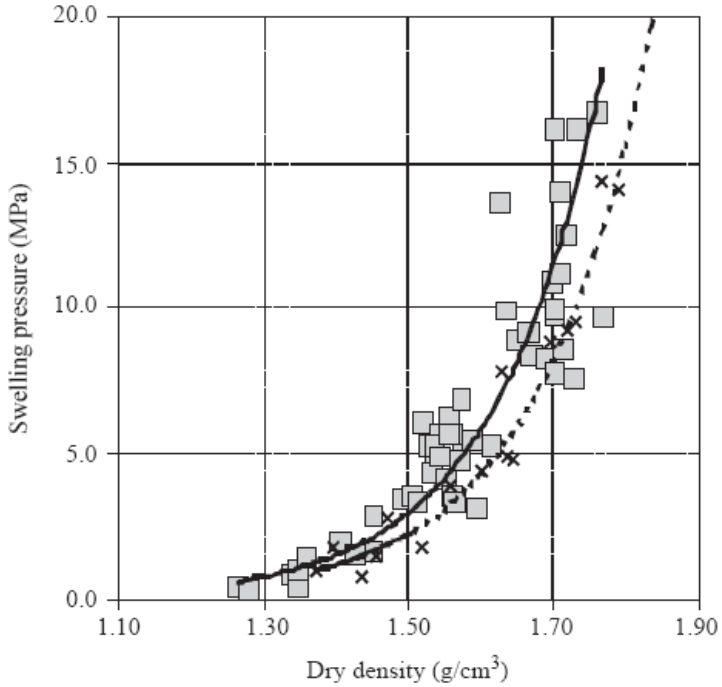

Figure 2-6. Swelling pressure of FEBEX bentonite (square dots). Crosses correspond to the ‘‘S-2’’ bentonite (Alonso et al. 2005).

2.3.2 TOUGHREACT-FLAC simulation results

The swelling stress experiments were simulated using a 3D 20×20×20 mm model with 20 elements in the vertical direction (Figure 2-7). The model boundaries are fixed for displacement normal to the boundaries, which means that the model is fully confined from a mechanical perspective. The model is also hydraulically confined (no flow across boundaries) except at the bottom (water inlet) where a fully saturated condition is applied. The simulation wasconducted for about 10 days under isothermal conditions at a temperature of 25°C.

Those nonboundary gridblocks have an initial saturation degree of 65%, which corresponds to a gravimetric water content of about 14%. Obtaining the chemical composition of pore water for a bentonite sample with such low water content is challenging (Sacchi et al. 2001, Zheng et al. 2008), and different measurements and numerical interpretation methods lead to different pore-water chemical compositions (Fernandez et al. 2001, Zheng et al. 2008). In this report, the initial chemical composition for unsaturated bentonite is taken from Fernandez et al. (2001), which is listed in Table 1. A fully saturated condition is applied to the gridblock at the bottom boundary, and the chemical composition on this gridblock is taken from Zheng et al. (2010). Zheng et al. (2010) presented a heating and hydration experiment in FEBEX clay. The clay samples were hydrated with distilled water, and part of the sample became fully saturated. We therefore took the chemical composition of the pore water for the fully saturated sample and apply to the gridblock at the bottom boundary.

Table 2-1. Initial pore water composition (mol/kg except for pH) in non-boundary and bottom boundary gridblocks.

	nonboundary	bottom boundary
pH	7.72	7.60
Cl	1.60E-01	8.26E-03
SO_4^{-2}	2.12E-02	9.49E-03
HCO_3^-	5.01E-04	3.57E-03
Ca^{+2}	1.13E-02	2.23E-03
Mg^{+2}	1.44E-02	2.36E-03
Na^+	1.88E-01	3.44E-02
K^+	1.68E-03	5.03E-04
Fe^{+2}	2.86E-09	2.86E-09
SiO_2(aq)	3.37E-04	3.37E-04
Ionic strength	0.25	0.045

Figure 2-7 shows a plot of the saturation distribution after about 4 days. In the simulation, the soil sample becomes practically fully saturated in about 7 to 9 days (Figure 2-8). As the soil sample is hydrated from the bottom, the ion concentration, represented by ionic strength, decreases gradually (Figure 2-9).

When a linear elastic model such as described by Equation (2-6) is used, Rutqvist et al. (2011) calibrated the moisture swelling coefficient as 0.238, leading to a maximum value of about 5.56 MPa, which is higher than the expected 5 MPa (Figure 11 solid lines). The reason for this is that gas is trapped and gas pressure increases by about 0.5 MPa, creating an additional stress increase of about 0.5 MPa (Figure 2-10). The effect of gas pressure on stress can be eliminated by setting Biot's constant to a very small number e.g., 1e-10. In such a case, the final stress is 5.12 MPa, i.e., exactly 5 MPa above the initial stress of 0.12 MPa (Figure 2-11 dashed line).

When a linear elastic model with chemically induced swelling such as described by Equation (2-7) is applied, we expect that Equation (2-7) could lead to results similar to those found using Equation (2-6) (Figure 2-11 solid lines), except that the moisture swelling coefficient has to be recalibrated. Figure 2-12 shows that a similar results can be obtained using Equation (2-6) (Rutqvist et al. 2011) and Equation (2-7), although significant differences are observed for some early times. The newly calibrated moisture swelling coefficient is 0.187, and the chemical swelling coefficient is calculated by Equation (2-5). Note that the effect of gas pressure on stress is not corrected in this calculation.

To illustrate the contribution of chemically induced swelling, we conducted a simulation based on Equation (2-6) using the moisture swelling coefficient of 0.187 (Figure 2-13). The chemically induced swelling accounts for about 20% of the total swelling stress.

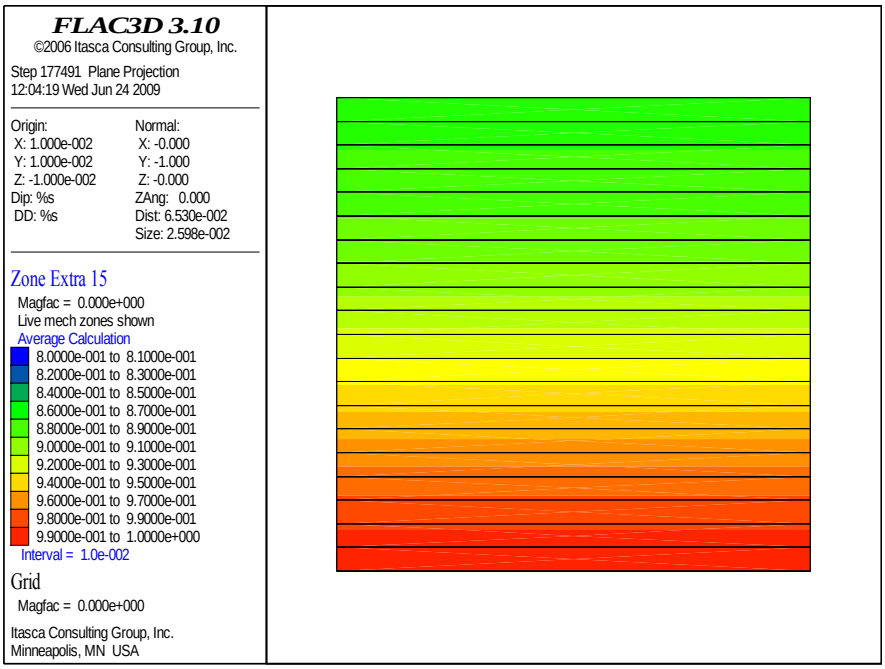

Figure 2-7. Plot of saturation contour after 4 days.

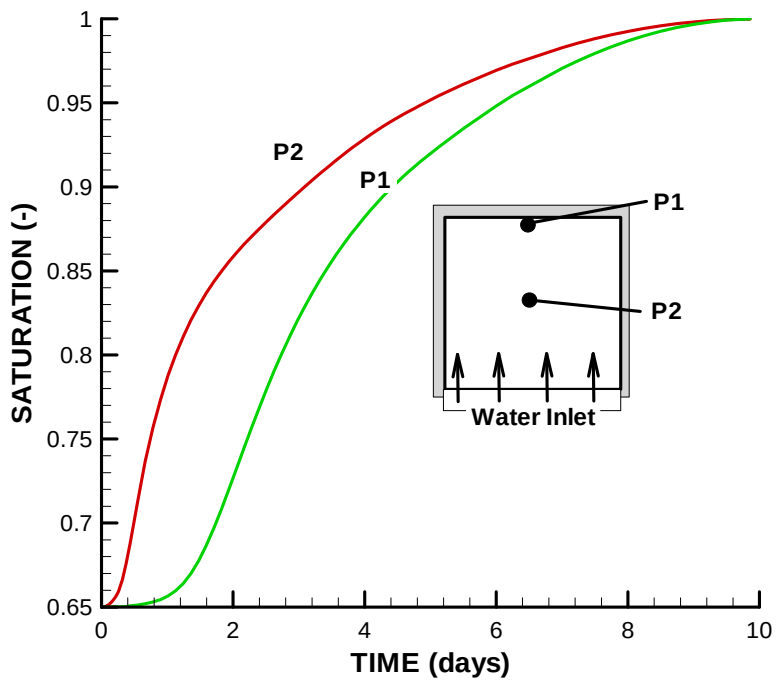

Figure 2-8. Evolution of saturation over time at the upper end of the model.

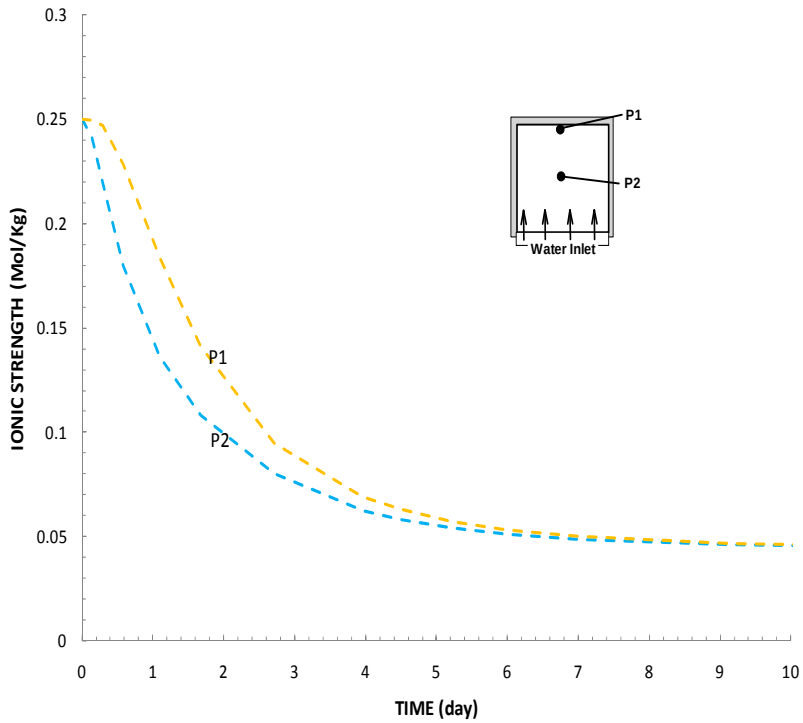

Figure 2-9. Evolution of ionic strength over time at the upper end of the model.

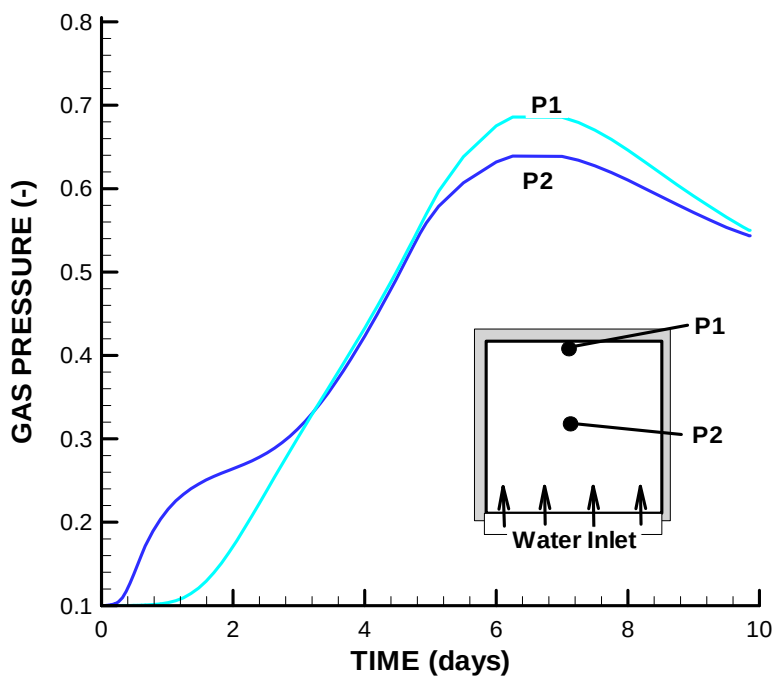

Figure 2-10. Evolution of gas pressure over time at the upper end of the model.

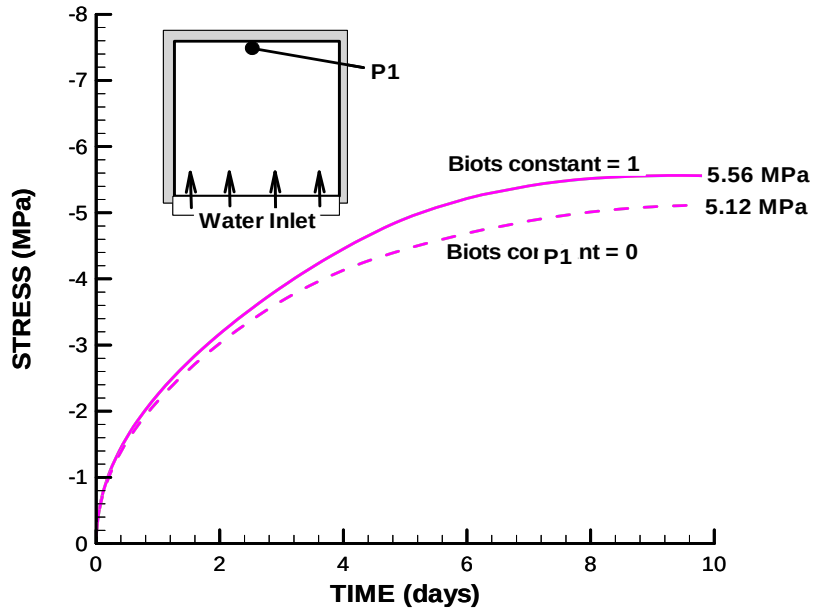

Figure 2-11. Evolution of compressive stress over time for the linear elastic swelling model (Rutqvist et al., 2011).

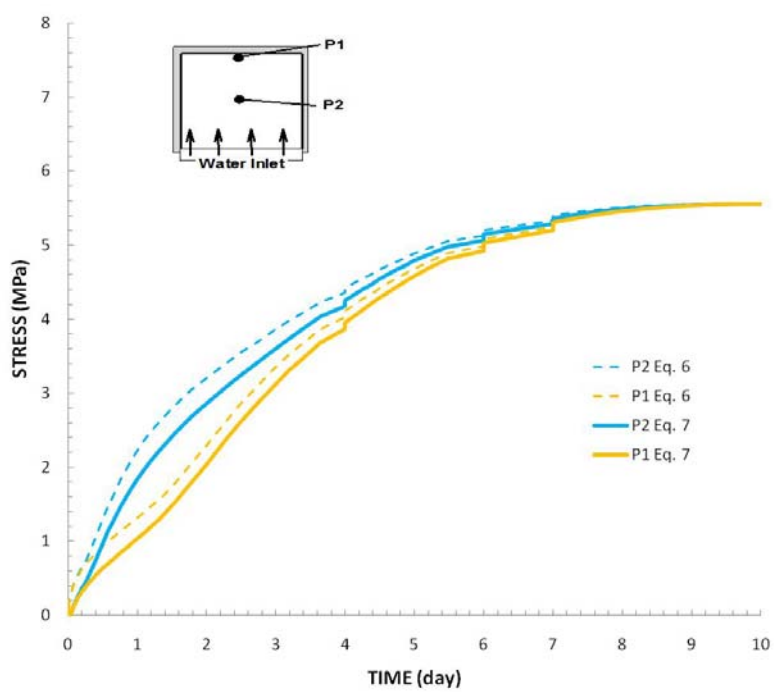

Figure 2-12. Evolution of compressive stress over time, calculated with Equation (2-6) with a moisture swelling coefficient of 0.238 (Rutqvist et al., 2011), and Equation (2-7) with a moisture swelling coefficient of 0.187 and a chemical swelling coefficient based on Equation (2-5).

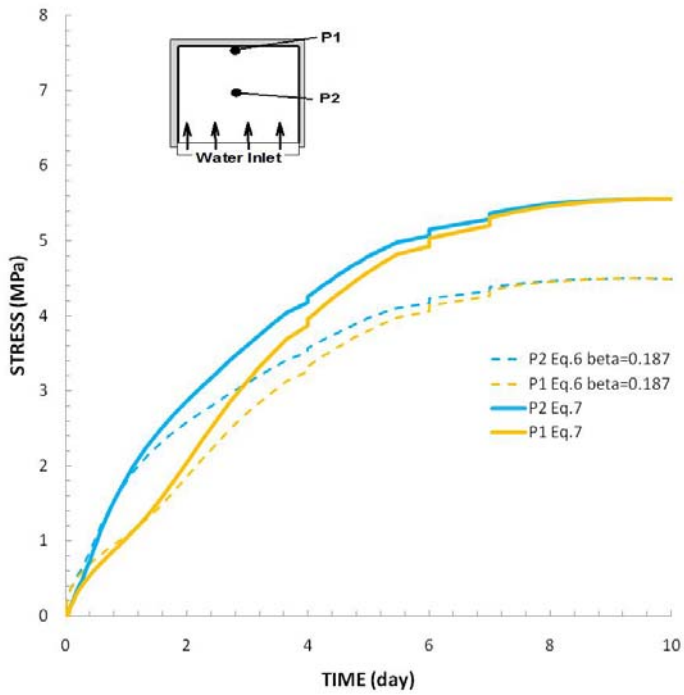

Figure 2-13. Evolution of compressive stress over time, calculated with Equation (2-6) with a moisture swelling coefficient of 0.187 and Equation (2-7) with a moisture swelling coefficient of 0.187 and a chemical swelling coefficient based on Equation (2-5)..

2.4 Conclusions and Future work

We have presented the status of development for a coupled THMC model using TOUGHREACT-FLAC. The following progress has been made to date:

- TOUGHREACT-FLAC has been linked to provide the necessary numerical framework for fully coupled THMC modeling.
- The TOUGHREACT-FLAC simulation approach has been demonstrated and tested for modeling bentonite swelling as a result of changes in saturation and pore-water composition, using a simple linear elastic swelling model.
- An approach for more rigorous swelling modeling has been identified, based on linking the diffuse double layer (DDL) theory for swelling to a geomechanical double structure model involving micro- and macro-structural changes.

Next steps in this development include:

- Continue extension of the existing implementation of the Barcelona Basic Model (BBM) to the double structure behavior equivalent to the Barcelona Expansive Model (BExM). This will be conducted within the UFD EBS work package.

- Develop the necessary links between DDL and BExM models for rigorous (mechanistic) modeling of the swelling phenomena.
- Implementation of the model within the TOUGHREACT-FLAC numerical framework.
- Testing and demonstration of the new model capability using published experimental data.

A variation on this approach will also be applied to clay host rock, such as shale layers.

3. DISCRETE FRACTURE MODELING FOR A DISTURBED-ROCK ZONE IN A CLAY REPOSITORY

3.1 Disturbed-Rock Zone (DRZ) Fracturing

The DRZ is the zone around repository excavations wherein the surrounding rock has been mechanically affected by the presence of the excavation openings and/or changes induced by operational factors. The most significant change caused by these kinds of disturbances is the potential development of an interconnected fracture network. The presence of such a network could lead to an increase in hydraulic conductivity and preferential flow along repository excavations from waste emplacement tunnels, through access tunnels, to the accessible environment. Such changes could lead to the creation of fractures that could degrade the favorable low-permeability characteristic of the clay/shale host rock. Observations in European underground research laboratories have shown that DRZ fracturing occurs locally around excavations in various argillaceous rock environments. These observations include both soft-clay formations (Boom Clay at Mol, Belgium) and more indurated clay formations (Callovo-Oxfordian at Bure, France and Opalinus Clay at Mont Terri, Switzerland).

The evolution of the DRZ can be subdivided into four stages, based on operational considerations (Tsang et al. 2010): (1) construction; (2) ventilation; (3) waste and backfill emplacement; (4) postclosure. The DRZ represents a region of enhanced permeability resulting from porosity increase or creation of tensile or shear fractures. Above and below the excavation, fractures tend to occur along bedding planes, while laterally along the excavation, layers of vertical fractures can form. The DRZ is generally about one drift radius thick, with an initial increase in permeability of as much as five orders of magnitude has been found (Tsang et al. 2010). However, the enhanced permeability effect decreases over time because of clay swelling and clay creep behavior, especially in cases where steel support and concrete lining provide a back pressure on the rock (Tsang et al. 2010).

Ventilation begins immediately following excavation and continues until emplacement of waste and backfill. Tensile stresses develop during ventilation as a result of rock shrinkage caused by dryout (Tsang et al. 2010). The shrinkage is the response of expandable clay interlayers to dehydration as well as associated increases in pore-water ionic strength upon drying. Clay minerals are composed of negatively charged sheet silicates bound together by hydrated interlayer cations. The higher ionic strength of the pore water induces a chemical

gradient between waters of hydration in the clay inter-layers and the pore water, leading to migration of the interlayer water into the pores. This causes the interlayer distance to decrease and the clay to shrink macroscopically. The impact of ventilation on the rock will be affected by the type of ground support used, which may take the form of a lining covering the majority of the tunnel surface. The drying of the clay can lead to an increase in the mechanical strength of the rock, a result of the smaller interlayer distance (Morrow et al. 2000), as well as the reduction in pore pressure (Tsang et al. 2010).

Drying and dessication cracking can occur following emplacement of waste and backfill as a result of the waste heat. Differential thermal expansion and pore-pressure buildup can also lead to changes in compressive and tensile stresses and chemical reactions. The thermal effects will continue, but eventually dissipate during the postclosure period. Water that has been lost during previous operational phases by ventilation and heating will start to return and resaturate the DRZ. Swelling, enhanced creep, and fracture self-sealing are expected to play an important role relative to the behavior of flow in the DRZ.
The main features of DRZ fracturing have been reported by Lanyon and Senger (2011). Geomechanical modeling, laboratory testing, and fracture mapping in Mont Teri tunnels indicate that the following disturbances are likely: (1) extension (unloading) fractures in a narrow zone near the tunnel side-walls; (2) disturbed bedding planes within buckling zones above and below the tunnel; (3) bounding and internal shear fractures around and within the buckling zones.

An important issue associated with DRZ fracturing is the extent and connectivity of the fractures. Lanyon (2007) evaluated fracture length, orientation, and density for several modes of fracturing expected in the DRZ environment. Extension fractures are formed normal to the minimum principal stress and are subparallel to the tunnel side walls. Borehole cores into the side walls of a 2.5 m diameter tunnel at the Mont Teri URL indicate that extension fractures are limited to fracture lengths of about 1 meter. Transmissive extension fractures lie within about a one-half tunnel radius of the tunnel wall. Fracture densities are less well characterized, but values of 1 to 2 m^2/m^3 have been used in modeling. Bedding-plane fractures within the buckling zones are oriented mainly by the geometry of the depositional beds. The bedding planes are continuous over large distances, but slight misorientations between the tunnel and the bedding planes or other factors, such as heterogeneity in the bedding plane reactivation caused by buckling, are expected to limit the continuity of the feature. Lanyon (2007) used a fracture length of 10 m for bedding plane fractures. Geomechanical modeling indicates that the buckling zone may extend 3 tunnel radii from the tunnel wall, and that spalling thickness may scale as one-tenth of the tunnel radius. The bounding shear fractures form the boundaries of the buckling zones above and below the tunnel, and are subradial to the tunnel. Internal shear fractures also pass through the buckling zones subparallel to the bounding shear fractures and subradial to the tunnel. Because the buckling zone is continuous along the entire length of the tunnel, Lanyon (2007) states that the continuity of these features may possibly extend over the full length of the tunnel, but are also possibly disrupted, forming shorter features, by heterogeneity in the geomechanical properties of the rock. These features extend into the rock over the same dimensions identified for bedding-plane fractures associated with the buckling zones.

The DRZ is also impacted by natural features of the clay host rock, including sedimentary bedding planes and tectonic shear zones (also referred to as faults). Yong et al. (2010) investigated the development of induced fracturing in the Opalinus Clay at Mont Terri. Tectonic shears were found to influence induced shear fractures along the excavation side walls in terms of their location and orientation. The influence of natural features on DRZ fractures was also found by Nicollin et al. (2010). Resin injections used to impregnate the fracture network behind the gallery face before excavation were found to follow flow paths along pre-existing tectonic fault fractures. The DRZ fracture network was found to consist mainly of reactivated pre-existing tectonic fault fractures. New DRZ fractures were not common and led to the conclusion that DRZ characteristics are strongly influenced by tectonic features, in addition to stratigraphic properties, bedding directions, and stress perturbations produced by the excavation.

3.2 Potential Need for a Discrete Fracture Model to Represent the DRZ

A principal issue for flow and transport through any fracture system in a low-permeability rock is the connectivity of the fracture network. Fluid flow and transport pathways can be strongly influenced by the specific fracture-network connectivity for systems in which the fracturing is sparse and the associated network connectivity is limited. In these cases, a continuum model of a fracture network cannot reproduce the actual behavior, because continuum models of fracture networks are based on the assumption of complete connectivity at all scales. Discrete fracture-network models capture the network connectivity explicitly, which is particularly important when such connectivity imposes strong limitations on the flow system. Furthermore, because discrete fracture models do explicitly account for fractures, many types of geological and geophysical data can be more easily represented in the models. For the case of the DRZ, the effects of specific fracturing patterns that have been recognized through field observations and geomechanical modeling can be more easily incorporated in a discrete fracture network model for flow and transport processes.

In addition to direct implementation, discrete fracture network models may be used as a tool for calibration of fracture-network continuum models, as presented by Lanyon and Senger (2011). This requires an upscaling step in which properties from the DFN are “converted” to equivalent properties for a heterogeneous porous medium. Some of the difficulties involved in upscaling are discussed by Jackson et al. (2000). For example, consider a fracture with known characteristics that crosses a numerical grid. The actual effective porous-medium permeability is not solely a function of the local fracture properties within a particular grid, but is also affected by the fracture connectivity and properties of other fractures within the overall network. Therefore, the local equivalent porous medium permeability can be affected by nonlocal information about the fracture network.

3.3 Previous Discrete Fracture Network Modeling of the DRZ

Only one study of single-phase flow in a discrete fracture network associated with the DRZ has been documented. Lanyon (2007) conducted flow simulations for the DRZ based on characterization of DRZ fractures from the Mont Terri Underground Rock Laboratory. Lanyon's model used a discrete fracture approach and four types of fractures were considered—unloading joints, disturbed bedding, highly disturbed bedding, and shears, as discussed above. The highly disturbed bedding is the same configuration as disturbed bedding, but closer to the drift. Differences in mean conductivity and connectivity for fractures in these different categories were used to develop four variant cases. A hydraulic gradient of 0.25 was used (100 m drop in head over 400 m of tunnel). The results show that the average permeability of the DRZ was found to vary from about 10^{-16} to 10^{-15} m^2. This is significantly higher than the undisturbed clay matrix, which has a permeability range of 10^{-19} to 10^{-21} m^2. This enhanced permeability was found to be controlled mainly by the assumed frequency and transmissivity of the fractures. The model was used to determine the flow distribution in which flow was found to be concentrated in the buckling zones that lie above and below the drift. Relatively small amounts of flow moved through the unloading joints along the sidewalls of the tunnel.

3.4 Technical Developments and Issues for DFN Modeling

A major problem for the use of discrete fracture models is the construction of a suitable numerical mesh. Erhel et al. (2009) have found that the direct application of mesh generation is generally not successful, because of the complexity of fracture configurations and complex intersections. The unstructured nature of a stochastic fracture network leads to difficulties in the generation of a mesh that follows constraints required for the application to flow and transport modeling. For example, in the integrated finite difference method (Narasimhan and Witherspoon 1976), the ideal grid contains internodal connections that are orthogonal to cell boundaries and cross cell boundaries close to the middle of the boundary. For the finite element method using triangular elements, the ideal grid consists of triangular elements that do not contain small angles (Erhel et al. 2009). A number of issues concerning mesh generation for discrete fracture models have been identified by Reichenberger et al. (2006): (1) fracture intersections, where one fracture end protrudes only slightly from the intersection; (2) almost meeting fractures, where one fracture ends in close proximity to the other; (3) parallel fractures very close to each other; (4) fractures intersecting at a very small angle.

The problem with unconstrained stochastic discrete-fracture models is that complex geometrical anomalies such as those identified by Reichenberger et al. (2006) will cause difficulties in producing a suitable grid. This leads to the idea of restricting the degrees of freedom in defining the stochastic discrete-fracture network. Leckenby et al. (2007) compared well-test flow responses for fractured rock using regular discrete-fracture networks having constant fracture length, spacing, and orientation with stochastic discrete-fracture networks. The results led Leckenby et al. (2007) to the conclusion that the overall trends for flow through stochastic networks can be approximated by regular models. A

regular grid was also used for representing a discrete fracture network for geothermal analysis (Kolditz 1995).

These results suggest that constrained, stochastic discrete-fracture networks should be investigated as part of a modeling methodology for discrete fracture-network models of flow and transport processes. A potential simplification along the lines of the regular grid investigated by Leckenby et al. (2007) is to specify a discrete fracture network that is limited to discrete, deterministic fracture orientations. Orientations would be restricted to avoid small-angle fracture intersections. Similarly, fracture spacing within a given orientation would be limited to avoid extremely small spacings between parallel fractures. However, fixed-orientation fractures within a fracture set would have fewer fracture-fracture connections than in a fracture set with stochastic orientation. Therefore, fracture connections within a fracture set would need to be amended according to the estimated geometric variability in orientation within the fracture set. Further constraints could be used to avoid other geometric anomalies, including fractures that almost intersect and fracture intersections with negligible penetration. Although orientations would be deterministic, this method could include stochastic and heterogeneous fracture density, fracture length and width, and fracture hydraulic properties.

An alternative approach using hybrid finite element and finite volume methods has been developed, as described by Paluszny et al. (2007) and Matthäi et al. (2009). The method employs mixed tetrahedral-hexahedral finite element shapes, where complex geometrical surfaces are gridded using tetrahedrons with hexahedrons for geometrically unconstrained regions and for large-aspect-ratio geometries such as fractures, faults, and thin bedding. A finite element method used to solve for pressure response is coupled with a finite volume method for calculating flow and transport processes. The finite volume method requires specification of a second complementary grid consisting of node-centered finite volume elements. The finite volume grid is constructed using a barycentric tessellation of the finite element grid. The method encounters difficulties representing sharp changes in material properties along interfaces, because the dual-grid approach tends to smear out the effects of the property discontinuities in the finite volume gridding. However, an enhancement of the gridding method using additional nodes at material interfaces has been proposed to resolve the issue (Nick and Matthäi, 2011a,b).

One method for generating an unstructured mesh is known as Voronoi tessellation. A Voronoi tessellation partitions a spatial domain containing a set of nodal points into a set of spatial regions or cells, where each cell is associated with an individual nodal point. The defining characteristic of the Voronoi cell is that all locations within the cell lie closer to the associated nodal point than to any other nodal point. A particular Voronoi cell can then be constructed from the intersection of half-spaces delineated by the perpendicular bisectors of each internodal line segment drawn between the cell's internal node and remaining nodes in the domain. The Voronoi cell partitioning is unique, and results in a set of convex polygons in 2D or convex polyhedrons in 3D that fill the domain (Sukumar 2003). The Voronoi tessellation is locally orthogonal because the inter-nodal line segments are orthogonal to the corresponding bisecting line or plane that forms the cell interface.

The use of Voronoi tessellation as a gridding method for discrete fractures in two-dimensional systems has been investigated by Syihab (2009) for problems in petroleum recovery from fractured reservoirs. The representation of fractures is accomplished using a linearly oriented triplet of closely spaced nodes along the fracture. Each triplet of nodes consists of a middle node that lies on the fracture and two nodes that lie equidistant on each side of the fracture. A linearly oriented series of such nodal triplets can be used to construct a Voronoi cell that coincides with the location of a fracture as shown in Figure 3-1. In the approach used by Syihab (2009), fractures are not treated as reduced dimensional features. In other words, the fracture aperture is explicitly represented. Syihab (2009) also presents gridding techniques used for intersecting fractures based on a Voronoi method. However, ways to represent fractures and fracture intersections for three-dimensional Voronoi grids require further development. A simple two-dimensional, two-fracture, and matrix Voronoi grid is shown in Figure 3-2. This method for discrete fracture network gridding is analogous to the method used to represent discrete faults in the site-scale unsaturated flow model for the Yucca Mountain Project, which was also based on Voronoi gridding, as shown in Figure 3-3. Note that Figure 3-3 presents a two-dimensional plan view, which is a horizontal cross section from a three-dimensional grid.

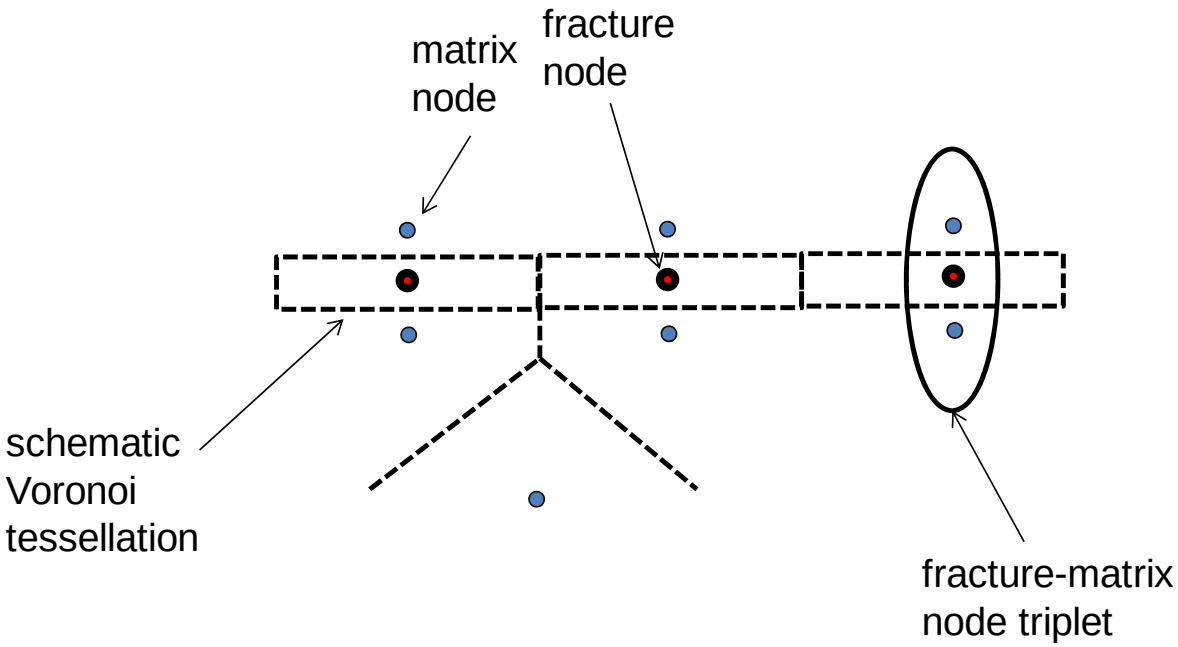

Figure 3-1. Voronoi nodes for discrete fracture and matrix model.

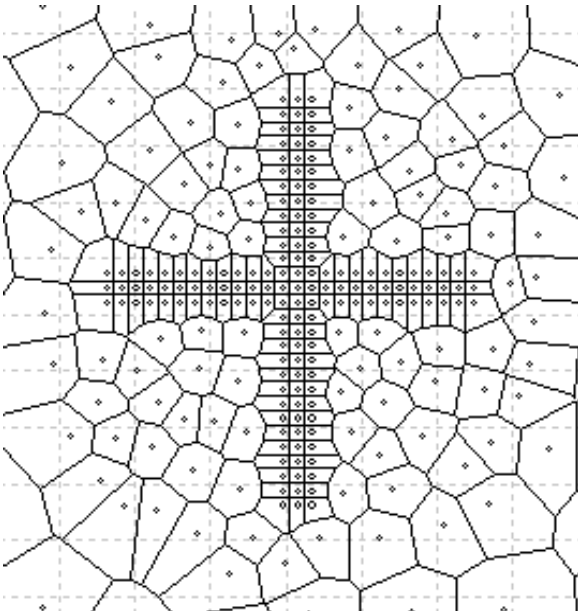

Figure 3-2. Discrete fracture grid using Voronoi gridding (modified from Syihab, 2009).

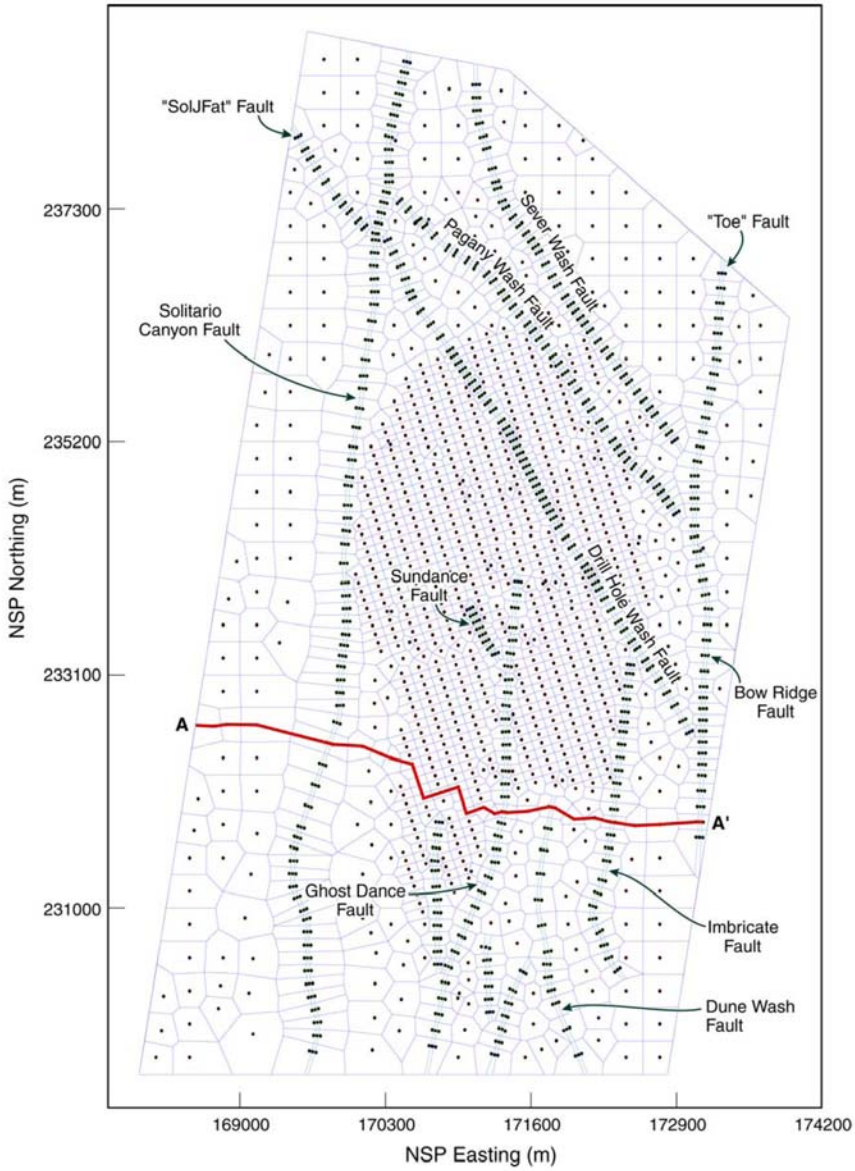

Figure 3-3. Plan view of the three-dimensional site-scale model for unsaturated zone flow at Yucca Mountain (BSC 2004).

Efficient construction of Voronoi grids from a given a set of nodes is an ongoing subject of research in computational geometry. A number of different algorithms have been developed that work on two-dimensional problems for small numbers of nodes. However, highly-efficient algorithms for large numbers of nodes in three dimensions generally run into problems as a result of degenerate nodal placement (such as five nodal points that are co-spherical) and/or errors caused by finite precision arithmetic (Ledoux, 2007). Direct construction methods are more robust but suffer from inefficiencies, limiting their use for large problems having unconstrained spatial distributions of nodes. By placing constraints on the maximum distance from any point to a node, it may be possible to partition the

problem such that less efficient but more robust methods can be used to compute the Voronoi cells in a manner amenable to parallel processing.

Another possible approach uses discrete Voronoi gridding. For this computational scheme, the entire domain is first tessellated into a set of small regular cells called voxels. The voxels are then assigned to Voronoi nodal points to create the discrete Voronoi grid. As for exact Voronoi gridding methods, there are tradeoffs between algorithm robustness and efficiency (van der Putte, 2009). However, algorithm simplicity and robustness appear to be advantages of the discrete Voronoi gridding method. One complication for the discrete voxel approximation is the proper assignment of internodal interface areas, because voxel interfaces areas are biased to values larger than the true interface areas.

3.5 Future Directions

Because the DRZ represents a restricted volume domain with particular fracturing patterns, a more direct approach for modeling flow through discrete fractures in the DRZ may be feasible than for the general problem of flow through discrete fracture networks. Items that need to be further investigated include the use of constraints for fracture network geometry, the use of full- or reduced-dimensional representations of fractures, and Voronoi gridding methods in three dimensions.

4. EXPERIMENTAL STUDY OF URANIUM DIFFUSION IN CLAY-RICH ENVIRONMENTS AND BENTONITE

4.1 Background and Research Objectives

The long-term management of nuclear waste repositories requires reliable predictions of contaminant transport in the subsurface at chemical conditions varying over time and space. This includes an evaluation of radionuclide mobility through waste containment barriers close to the source term. Compacted bentonite has been proposed as a backfill material for repositories due to its low permeability (Pusch, 1992; Kim et al., 1993; Bourg et al., 2003) and strong sorptive properties (Eriksen et al., 1999; Ochs et al., 2001). The limited permeability of bentonite is at least partially the result of its low porosity and the swelling of Na-montmorillonite, its major component, in water.

The transport of radioactive contaminants through bentonite layers is expected to be very limited and dominated by diffusion processes (Madsen, 1998; Ochs et al., 2001; Bourg et al., 2007). Hence, laboratory diffusion testing is an important component for the design of waste containment barriers (Shackelford, 1991), and for the calibration of diffusion-based transport models. Besides waste containment barriers, diffusion processes are also relevant under the following conditions: (1) in small-scale and/or longer-term transport in slow advection or water-stagnant zones (Bai et al., 2009); (2) in intragranular regions of

sediments and regions of low permeability, such as rock matrices or strata of fine-grained sediment (Bai et al., 2009); and (3) in the context of U(VI) mineral precipitates, e.g. at the Hanford site (Liu et al., 2006; McKinley et al., 2006).

As the basis of nuclear fuel, uranium is one of the primary elements to be considered in environmental risk assessments for nuclear waste repositories. Furthermore, other radionuclides that are bound in the fuel matrix can only be released at the same rate as uranium dissolves and diffuses through waste containment barriers (Muurinen, 1990). Hence, a fundamental understanding of uranium diffusion through bentonite is essential for environmental risk assessments. In addition, in conceptual diffusion studies, uranium can serve as a useful 'analog' for other radioactive contaminants, such as Pu, Np, and Am for numerous reasons. First, uranium is a radionuclide, which forms a variety of solution complexes with inorganic ligands that are relevant for the pore water chemistry of bentonite (Wersin, 2003; Joseph et al., 2011), such as carbonates, hydroxides, sulphates and chlorides (Guillaumont et al., 2003). At the same time, uranium redox chemistry is far less complex, e.g. in comparison to plutonium, with only two dominant oxidation states (U(IV) and U(VI)), which largely simplifies experimental setups and controls. Furthermore, a well-established thermodynamic database is available (Guillaumont et al., 2003), which is not the case to the same extent for other radioactive contaminants (e.g., Pu). In addition, uranium provides a good example of a contaminant, for which metal interactions with mineral surfaces are highly dependent on metal solution speciation and chemical solution conditions. Conveniently, at this point far more literature data are available regarding uranium surface interactions with clays compared to other radionuclides (154 reference 'hits' in the Web of Science, compared to 37, 24 and 22 for Pu, Np and Am; 7-22-2011).

The primary goal of this study is to characterize the effects of uranium(VI) solution speciation on apparent uranium diffusion rates in compacted bentonite. Various types of diffusion coefficients are usually distinguished in the context of metal transport in porous media including: 1) molecular diffusion coefficients describing chemical diffusion in aqueous solution; and 2) apparent diffusion coefficients, which additionally take into account some or all effects of the solid phase. The latter effects are caused by the tortuosity of the porous network, and a variety of metal-mineral interactions, such as surface complexation, ion exchange, etc. Both molecular and apparent diffusion coefficients can be affected by metal solution speciation and chemical solution conditions, such as pH and aqueous carbonate concentrations. Specifically for clays, it is understood from both modeling and experimental studies that diffusion processes are influenced by: 1) the electrical charge of the diffusing solute, 2) the degree of compaction and the number of interlayer water molecules in the clay structure, and 3) the electrical double layer structure at the clay/water interface. However, most currently available uranium diffusion

coefficients do not specifically account for the effects of metal solution speciation or clay characteristics on molecular or apparent diffusion rates. Clearly, a 'de-coupling' of parameters and processes is necessary in order to ensure the accurate prediction of apparent diffusion rates at chemical conditions changing over time and space. Predictive models need to allow for a clear distinction between metal diffusion and sorption reactions, and specifically take into account the individual effects of solution speciation on each of these processes.

In this study, we will use a series of lab-scale experiments to evaluate the effects of chemical solution conditions on apparent uranium diffusion rates, and to provide input data for later simulations. Overall, this will contribute to an improvement of the predictive capabilities of diffusion-based transport models, and deepen our conceptual understanding of the underlying physico-chemical mechanisms of diffusion.

4.2 Diffusion in Porous Media and Types of Diffusion Coefficients

In this section, we provide a brief overview of the most relevant types of diffusion coefficients used for solute transport in aqueous solution and saturated porous media. This is followed by a brief discussion of equations relevant for metal diffusion in porous media.

4.2.1 Molecular Diffusion Coefficients

Molecular diffusion is defined as solute transport due to the random thermal motion of molecules in solution (Selim et al., 1997). In liquids, the Stokes-Einstein equation is the most common basis for the estimation of molecular diffusion coefficients (D_0) (Cussler, 1997).

$$D_0 = \frac{k_B T}{f} = \frac{k_B T}{6\pi\mu R_0} \tag{4-1}$$

where f is the friction coefficient of the solute, k_B is Boltzmann's constant, T is temperature, μ is the solvent viscosity, and R_0 is the solute radius. This equation describes the diffusion of large solutes, in form of rigid spheres, through a continuum of small solvent molecules (Cussler, 1997). Strictly speaking, the Stokes-Einstein equation and all of its empirical extensions are limited to infinitely dilute solutions. However, diffusion coefficients in liquids are highly dependent on solute concentrations, often varying over several hundred percent while showing minimum and maximum values (Cussler, 1997). Hence, various researchers have been working on extensions of the

Stokes-Einstein equation to account for these concentration effects (Cussler, 1997); however, a detailed discussion of these approaches goes beyond the scope of this report.

Furthermore, the values of diffusion coefficients decrease with increasing solute radii. If the solute of interest is hydrated or solvated in any way, then the radius relevant for its diffusion characteristics is represented by the solute-solvent complex, and not the solute itself (Cussler, 1997). For instance, Zhou et al. (Zhou et al., 2002) reported that the hydration radii of Li^+ (3.10 x 10^{-10} m) and Na^+ (2.99 x 10^{-10} m) are increased in comparison to their respective Pauling radii (0.60 x 10^{-10} m for Li^+, and 0.95 x 10^{-10} m for Na^+), and argued that the mobility of these cations may be hindered by their first hydration shells, leading to lower diffusion coefficients.

Changes in chemical solution speciation may affect the molecular diffusion rates of uranium and other metals in the following ways. Uranium complexation with inorganic ligands, such as carbonates, can change the molecular size of uranium species, as well as its hydration properties and the water exchange kinetics with the hydration sphere (Kerisit et al., 2010). Current results from potential-based molecular dynamics simulations suggest that these changes lead to differences in molecular diffusion coefficients for various U(VI) solution species, e.g. between UO_2^{2+} and $UO_2(CO_3)_3^{4-}$ (Kerisit et al., 2010).

4.2.2 Effective Diffusion Coefficients

In porous media, migrating solutes experience tortuous pathways over increased transport distances. The effective diffusion coefficient (D_e) takes into account the tortuosity of the porous network (van Schaik et al., 1966), and is traditionally defined as

$$D_e = \tau D_0 \tag{4-2}$$

In principal, the tortuosity factor (τ) is a dimensionless, geometric parameter, but is likely to depend on water content (Selim et al., 1997), as well as clay compaction (dry density) and ionic strength conditions in the pore water (Van Loon et al., 2007). In addition, other factors can reduce the rate of diffusive transport of solutes in soil, such as: (1) the increased viscosity of the water adjacent to the clay mineral surface relative to the bulk water (e.g., (Kemper et al., 1964)), and (2) the exclusion of anions from the smaller pores of the mineral phases (e.g., (Porter et al., 1960)). At this point, the separation of the effects of geometry, fluidity, anion exclusion, etc. provides an ongoing challenge.

In addition to the effects described for molecular diffusion coefficients above, metal solution speciation may influence effective diffusion coefficients due to charge-related effects. In compacted bentonite, pore sizes can be so small that electric double-layers balancing the charge of the bentonite may overlap (Bourg et al., 2003; Bourg et al., 2006; Leroy et al., 2006; Kerisit et al., 2009). Furthermore, clay microstructures can change as a

function of bentonite compaction and ionic strength. The latter can lead to the co-existence of the diffuse double layer and bulk water, which in turn affects anion-accessible porosities in bentonite (Van Loon et al., 2007; Appelo et al., 2008). Overall, due to the complex charge distribution in bentonite pores, effective diffusion coefficients are most likely different for cations and anions as the principle of electroneutrality has to hold in micro- and macropore solutions. As a result, effective diffusion coefficients for uranium may become a function of the specific, molecular charge of individual uranium solution species. Hence, different diffusion coefficients have to be expected, e.g. for UO_2^{2+} and $UO_2(CO_3)_3^{4-}$. Muurinen (Muurinen, 1990) reported first indications of anion-exclusion effects for uranium in bentonite, and changes in effective diffusion coefficients due to differences in uranium speciation.

4.2.3 Apparent Diffusion Coefficients

For reactive solutes, such as uranium, metal interactions with the mineral surface in the pore environment have to be expected over the course of diffusion-dominated metal transport. As a result, some researchers have proposed the use of some form of an apparent diffusion coefficient (Maes et al., 2002; Tokunaga et al., 2004), which further extends the effective diffusion coefficient to directly include metal sorption or ion exchange reactions. For example, a simple apparent diffusion coefficient (D_a) can be defined as (Shackelford, 1991)

$$D_a = \frac{D_e}{R_f} \tag{4-3}$$

where R_f represents the retardation factor. In the simplest case, the retardation factor is based on a distribution coefficient (K_d), assuming linear, fully reversible sorption behavior

$$R_f = 1 + \frac{\rho_d}{\theta} K_d \tag{4-4}$$

where ρ_d is the dry (bulk) density of the soil, and θ the volumetric water content.

Chemical solution conditions and metal speciation are known to affect uranium sorption behavior to clays (Davis et al., 2004; Fox et al., 2006; Bradbury et al., 2011). Furthermore, Muurinen (Muurinen, 1990) reported changes in apparent diffusion coefficients due to differences in uranium speciation, and argued that different species appear to follow different diffusion mechanisms.

Hence, the direct incorporation of metal-mineral interactions into diffusion coefficients appears problematic for a variety of reasons. First, the overall values of apparent diffusion

coefficients become inherently dependent on and sensitive to the correct values of R_f. Hence, it becomes meaningless to report values of apparent diffusion coefficients of reactive solutes without a characterization of their sorption characteristics (Shackelford, 1991). Furthermore, at this point, most studies apply linear or non-linear isotherms to describe retardation factors. However, sorption isotherms are inherently dependent on the sorption characteristics of the solid phase, as well as on the concentrations and chemical solution speciation of the solute. Isotherms provide good estimates for specific system conditions or individual experiments, but do not allow for any predictions of contaminant transport behavior at chemical conditions changing over time and space. For example, based on simulations Brown et al. (Brown et al., 1991) demonstrated that the application of linear sorption isotherms for uranium sorption to London clay will be very limited. The value of R_f was shown to be highly dependent on uranium solution concentrations changing over space, even in the case of a 9 mm clay sample under controlled pH conditions (pH=8) at the lab-scale.

Furthermore, care has to be taken against the use of apparent diffusion coefficients in case of problems associated with flux-controlled boundary conditions (Rowe et al., 1988; Shackelford et al., 1991), since the effective diffusion coefficient, but not the apparent diffusion coefficient, is directly linked to diffusive flux.

Finally, extreme caution has to be exercised for the comparison of diffusion coefficients for reactive solutes between studies using various types of experimental setups (Shackelford et al., 1991). Errors may be introduced in the interpretation of results, if different types of diffusion coefficients are compared, or if different approaches have been taken to incorporate sorption characteristics into apparent coefficients.

4.2.4 Contaminant Transport Driven by Diffusion

The importance of a clear distinction of different types of diffusion coefficients becomes further apparent, when we evaluate the mathematical background of diffusion-dominated contaminant transport. The diffusive mass flux (J_D) of a non-reactive solute in saturated porous media is described by Fick's first law of diffusion

$$J_D = -D_e n \frac{\partial C}{\partial x} \tag{4-5}$$

where n represents porosity, C the solution concentration of a given species, and x space. Furthermore, Fick's well-known second law for the diffusion of non-reactive solutes in the 1-dimensional case states

$$\frac{\partial C}{\partial t} = D_e \frac{\partial^2 C}{\partial x^2} \tag{4-6}$$

where t is time. For reactive solutes interacting with the mineral phase, Equation (4-6) is further expanded to include the sorption term $\partial q / \partial t$

$$\frac{\partial C}{\partial t} = D_e \frac{\partial^2 C}{\partial x^2} - \frac{\rho_d}{\theta} \frac{\partial q}{\partial t} \tag{4-7}$$

Two principal approaches are possible to describe diffusion of reactive solutes. First, the sorption term in Equation (4-7) can be described by sorption isotherms, and then be combined with the effective diffusion coefficient to give an apparent diffusion coefficient. For example, assuming linear, reversible sorption reactions, the distribution coefficient (K_d) is defined as

$$K_d = \frac{q}{C} \tag{4-8}$$

and

$$\frac{\partial q}{\partial t} = K_d \frac{\partial C}{\partial t} \tag{4-9}$$

Substituting Equation (4-9) into Equation (4-7), and using the earlier definitions of the retardation factor (Equation (4-4)) and apparent diffusion coefficient (Equation (4-3)), this leads to

$$\frac{\partial C}{\partial t} = D_a \frac{\partial^2 C}{\partial x^2} \tag{4-10}$$

This approach of a combined treatment of metal sorption and diffusion has been used by a variety of researchers in uranium diffusion studies in the past (Yamaguchi et al., 1997; Yamaguchi et al., 1998; Rameback et al., 2000; Tokunaga et al., 2004). On the other hand, following a different approach, the sorption term in Equation (4-7) can be treated independently of the diffusion mass transfer, e.g. by including sorption isotherms or a surface complexation model. This strategy has been applied less frequently (Bai et al., 2009; Liu et al., 2010).

4.2.5 Proposed Approach: De-Coupling of Diffusion and Metal-Mineral Interactions

As described above, variations in chemical solution conditions and metal solution speciation may affect both, uranium sorption behavior (Davis et al., 2004; Fox et al., 2006; Bond et al., 2008) and uranium diffusion rates (Muurinen, 1990; Liu et al., 2010). However, the individual effects of metal solution speciation on sorption and diffusion processes are most likely inherently different. Hence, we propose a de-coupling of these processes in diffusion-dominated transport models. This will allow for a specific incorporation of the individual effects of solution speciation on each of these processes. Furthermore, we suggest the application of surface complexation models to directly link metal speciation with metal-mineral interactions.

As part of this study, a series of systematic experiments will be performed to characterize effects of solution speciation on the various types of uranium diffusion coefficients. This will provide input data for the development of new modeling frameworks in collaboration with other researchers (Carl Steefel, Ian Bourg, LBNL).

4.3 Typical Experimental Setups Used in Diffusion Studies

In general, there are two main categories of experimental setups used to determine diffusion coefficients (Shackelford, 1991): (1) steady state, and (2) transient (non-steady state) methods. This distinction is based on the type of transport equation that is used in the calculation of diffusion coefficients using experimental data and appropriate initial and boundary conditions. Transient methods can be further categorized into column methods, half-cell methods, and reservoir methods. In the following overview, we will briefly describe the general experimental setup for each type of method, discuss individual advantages and disadvantages, and provide examples from the literature for method applications.

4.3.1 Steady-State Methods

Steady-state methods allow for the determination of effective diffusion coefficients, since by definition there is no retardation of reactive species at steady-state (Shackelford, 1991). In this type of setup (Fig. 4-1a), the mineral phase is contained between two reservoirs (Shackelford, 1991). The source reservoir contains the solute of interest at an either measured or controlled concentration (high concentration C_1), the collection reservoir is used to periodically withdraw volume fractions for the analysis of solute concentrations (low concentration C_2). Due to the concentration gradient between the two reservoirs, the solute diffuses through the mineral phase into the collection reservoir. Once steady-state conditions have been reached, and mass changes per time increment are the same in both reservoirs, Fick's first law (Equation (4-5)) can be utilized to calculate the effective diffusion coefficient (Shackelford, 1991). Furthermore, at the end of the diffusion

experiment, the mineral phase can be sliced and characterized to determine concentration profiles (Fig. 4-1b). Diffusion coefficients can be calculated by using either external (solution concentration based) or internal (solid phase concentration based) concentration gradients. However, different values for diffusion coefficients have to be expected depending on the approach, e.g. if an assumption of a linear concentration gradient across the mineral is not justified due to coupled flow processes (Muurinen, 1990; Shackelford, 1991).

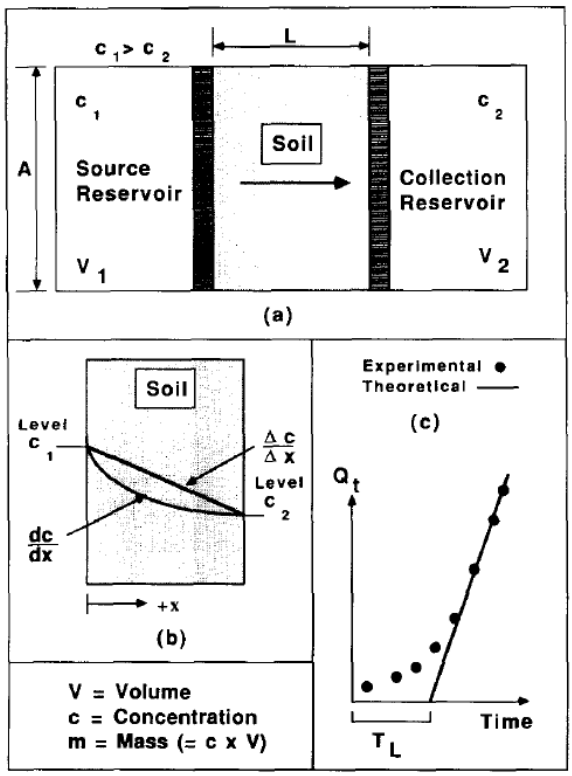

Figure 4-1. Overview of steady-state method: (a) diffusion cell; (b) concentration profiles in soil sample; and (c) time-lag method (Shackelford, 1991).

The main advantage of steady-state methods is that the effective diffusion coefficient (D_e) of reactive contaminants can be calculated without additional knowledge of their sorption characteristics and retardation factors. On the other hand, a large disadvantage is that typically long time-frames are required to reach steady-state. For instance, Muurinen (Muurinen, 1990) performed diffusion experiments over 150-200 days to characterize uranium diffusion through bentonite samples with a thickness of 7 mm. In addition, there is the need to maintain a constant concentration gradient over the course of the experiment by continuously replenishing lost solute in the source reservoir and removing received solute in the collection reservoir, e.g. in form of a flow-cell setup. The diffusion behavior

of uranium has been studied with steady-state methods previously (Muurinen, 1990; Yamaguchi et al., 1997; Yamaguchi et al., 1998).

The time-lag method is a slightly modified approach of the steady-state method, which allows for the calculation of apparent diffusion coefficients (D_a), provided that the retardation factors of the solute have been determined, e.g. in independent batch sorption experiments (Shackelford, 1991). In this case, the time-lag (T_L), the point where the asymptote of the breakthrough curve crosses the time axis (Fig. 4-1c), is used to determine the apparent diffusion coefficient (Muurinen, 1990). This approach still requires that steady-state conditions are reached during an experiment, but these conditions do not have to be further maintained for actual measurements. This is advantageous, since it helps to shorten overall experimental time-frames. On the other hand, this approach requires a determination of retardation factors for reactive solutes in independent sorption experiments. In addition, the limitations associated with the direct incorporation of sorption characteristics into diffusion coefficients, which have been described in detail above, also apply.

4.3.2 Transient Methods

Transient methods have been used to determine effective diffusion coefficients in the presence or absence of advective flow conditions (Shackelford, 1991), using column, half-cell or reservoir methods.

4.3.2.1 Column Methods

In context of diffusion experiments, column methods are used to determine effective diffusion coefficients based on the relationship between the hydrodynamic dispersion coefficient (D_h), the mechanical dispersion coefficient (D_m) and the effective diffusion coefficient, as described below (Equation (4-11)).

$$D_h = D_m + D_e \tag{4-11}$$

For this purpose, a constant solute concentration is often injected with the column influent, while effluent fractions are collected and further analyzed. From the results of the solute breakthrough curve, the hydrodynamic dispersion coefficient can be computed provided that the contaminant retardation factor is known. Alternatively, a non-reactive tracer can be used to determine D_h for the system while assuming $R_f = 1$. Then, if the mechanical dispersion coefficient is known, D_e can be back-calculated based on Equation (4-11). An alternate approach is to decrease the flow velocity so far that D_m can be neglected and D_e can be approximated by the value of D_h.

The primary advantage of column methods is that they represent a well-established approach. However, the mathematical separation of D_h, D_m and D_e involves multiple variables, which might lead to the propagation of errors. For example, this might be the case if a linear distribution coefficient is used, while the contaminant fraction sorbed is dependent on solute concentrations. As a result, the retardation factor used in calculations would not capture the non-linear sorption behavior of this contaminant. Up to this point, examples of the application of column methods for the determination of uranium diffusion coefficients have been fairly limited (Yoshida et al., 1991).

4.3.2.2 Half-Cell Methods

With half-cell methods, it is possible to determine apparent diffusion coefficients or effective diffusion coefficients, if the solute retardation factor is known. In this setup (Fig. 4-2), the experiment is started by connecting two half-cells containing the mineral phase. One of the two cells is tagged with a solute tracer, while the other one is initially free of the solute of interest. Due to the concentration gradient, solutes diffuse from the 'tagged' into the 'clean' cell over time leading to a change in concentration profiles in the solids packed into both cells. At given time-points or at the end of the experiment, the cells are disassembled, sectioned and characterized in terms of concentration profiles. Diffusion coefficients are then found by fitting the experimental data with analytical solutions to Fick's second law (Equation (4-10)).

The half-cell method represents a well-established setup, which has been applied by many soil scientists in the past (Shackelford, 1991). However, care has to be taken to ensure full contact between the two half-cells in order to avoid experimental artifacts. In the context of uranium diffusion, this approach has been used by Yoshida et al. (Yoshida et al., 1991), who combined the half-cell method with a column approach by percolating pore water through two combined clay cores. Furthermore, Rameback et al. (Rameback et al., 2000) used a similar approach to study uranium diffusion from a solid UO_2 fuel piece into bentonite.

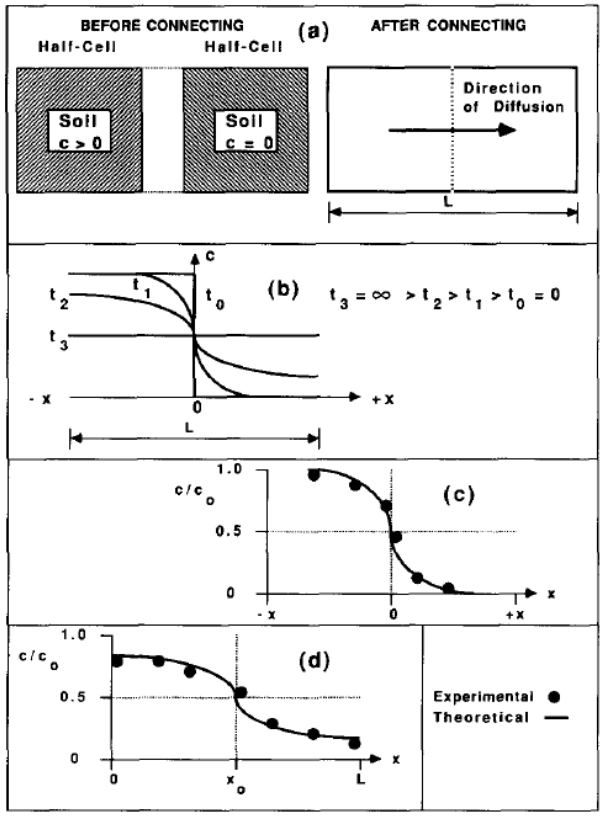

Figur 4-2. Half-cell method: (a) test set-up; (b) concentration profiles in soil; (c) profile for infinite medium; and (d) profile for finite medium (Shackelford, 1991).

4.3.2.3 Reservoir Methods

In reservoir methods, the solid sample is brought into contact with either one (single reservoir method) or two (double reservoir method) solution reservoirs in the absence of advective flow conditions. Either apparent or effective diffusion coefficients can be determined, as long as contaminant sorption characteristics and retardation factors are known.

In the double reservoir method, the source reservoir initially contains a known concentration of the solute, which decreases due to solute diffusion into the solid phase over the course of the experiment. The solute is then accumulated in the collection reservoir, from which it is periodically sampled. Hence, the double reservoir method is very similar to the setup of steady-state methods, except for the fact that solute concentrations in the reservoirs are not controlled to reach or maintain steady-state conditions. Diffusion coefficients are calculated based on contaminant concentrations in

reservoir solutions and/or the solid, determined under transient conditions. As a result, experimental time-frames can be substantially reduced compared to steady-state methods. According to our knowledge, there exists currently no example of uranium diffusion experiments utilizing the double reservoir method.

In the single reservoir method, the collection reservoir is absent and the solute concentration in the source reservoir is either held constant or allowed to decrease over time (Figs. 4-3 and 4-4). At the end of experiments, concentration profiles in the solid are used to calculate diffusion coefficients while considering appropriate initial and boundary conditions for the case of a semi-infinite or finite solid medium. If solute concentrations in the source reservoir are allowed to decrease over time, then effective diffusion coefficients can also be determined based on the profile of time-dependent solution concentrations.

One advantage of single reservoir methods is that complete solute transport through the solid sample is not necessarily required for data interpretation, which can again decrease the time-scale of experiments. However, the moisture content and saturation of samples have to be controlled in order to avoid experimental artifacts. This experimental approach has been utilized in various uranium diffusion studies before. For instance, Bai et al. (Bai et al., 2009) used an 'inward-flux' diffusion cell, which is comparable to a single reservoir method, except for the fact that the packed soil was exposed to a constant solute concentration at both ends of the packing. Liu et al. (Liu et al., 2010) set up multiple single cells in a large solution reservoir, which was spiked with U(VI) repeatedly to maintain constant solute concentrations. Tokunaga et al. (Tokunaga et al., 2004) combined a single reservoir method with X-ray microprobe and micro-XANES for the characterization of uranium concentration profiles and oxidation state in the solid phase.

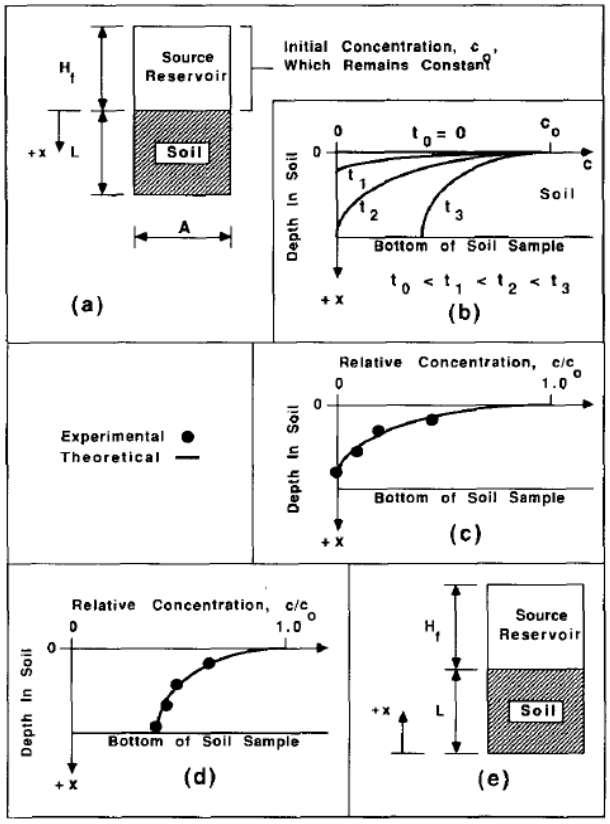

Figure4-3. Single reservoir method with constant source concentration: (a) test set-up; (b) concentration profiles in soil; (c) profile for semi-infinite medium; (d) and finite medium; (e) positive x-direction for finite medium case (Shackelford, 1991).

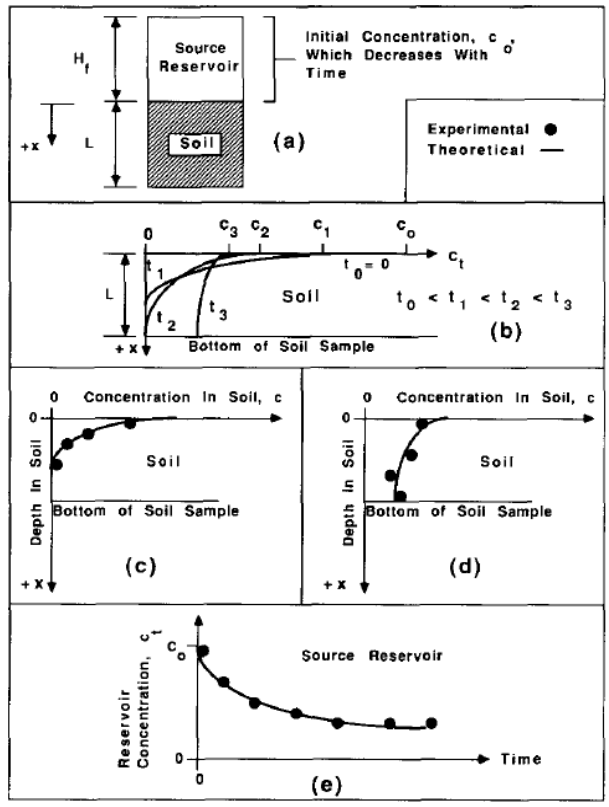

Figure 4-4. Single reservoir method with decreasing source concentration: (a) test set-up; (b) concentration profiles in soil; (c) profile for semi-infinite medium; (d) and finite medium; (e) concentration in source reservoir versus time (Shackelford, 1991).

4.3.3 Strategies for Sample Analysis and Characterization

In diffusion experiments, total metal concentrations and metal speciation need to be characterized in reservoir solutions and/or the tested mineral sample. Usually, this is done either continuously during, or at the end of an experiment. Uranium solution concentrations are often quantified in experimental reservoirs by using a radiotracer (U-233) combined with liquid scintillation counting (Yoshida et al., 1991; Maes et al., 2002), by kinetic phosphorescence analysis (KPA) (Tokunaga et al., 2004; Bai et al., 2009), or ICP-analysis (Tokunaga et al., 2004). Furthermore, electromigration appears be a useful technique to characterize dominant uranium solution species involved in diffusion processes (Maes et al., 2002).

The analysis of uranium concentrations in the solid phase usually requires some form of 'slicing' or preparation of thin sections (Muurinen, 1990; Yoshida et al., 1991; Bai et al., 2009) followed by metal extraction procedures and analytical measurements. For example, one approach for sectioning has been to quick-freeze the mineral phase, and to use a refrigerated microtome to partition the extruded solid into sections of up to 50 µm thicknesses (Barraclough et al., 1979; Shackelford, 1991).

After the preparation of thin sections, contaminants can be extracted from the solid phase based on three main methods (Shackelford, 1991): 1) high-pressure pore water squeeze (HPPWS) or centrifugation; 2) chemical extraction; and 3) chemical digestion. Both, centrifugation (Bai et al., 2009) and the HPPWS technique (Crooks et al., 1984; Johnson et al., 1989) are used to force the pore fluid out of the solid. It is assumed that the metal concentrations determined in the collected pore water represent free (liquid phase) concentrations, which have not been sorbed onto or associated with the mineral phase in any other form. Hence, these concentrations are directly linked to the effective diffusion coefficient without any further correction for metal sorption reactions based on retardation factors. In contrast to that, chemical extraction and digestion methods result in the measurement of the total (free and sorbed) metal concentrations, which need to be corrected with retardation factors if the goal is the determination of effective diffusion coefficients. A variety of chemical extractions procedures have been applied to remove metals for mineral phases in the past. For instance, uranium surface speciation has been qualitatively characterized in terms of metals involved in ion exchange reactions or associated with organics, carbonates and oxides (Yoshida et al., 1991). In case of chemical digestions, total metal concentrations do not only include mobile (sorbed and liquid phase) concentrations, but also nonmobile or residual fractions associated with primary and secondary minerals of the sample. While mobile metal concentrations can be calculated based on difference, uranium background concentrations in field samples and their potential contribution to mobile concentrations may complicate the data interpretation for both, chemical extraction and digestion methods (Bai et al., 2009).

An alternative to sectioning and extraction is the continuous characterization of the concentration profile in the solid, e.g. using autoradiographs combined with X-ray films (Evans et al., 1964). Similarily, the application of the Rutherford Backscattering Spectroscopy (RBS) technique may be specifically useful for the characterization of uranium diffusion behavior in consolidated clays or in granite fractures (Alonso et al., 2003; Alonso et al., 2003; Alonso et al., 2009). This technique allows for the measurement of uranium concentration profiles over short range distances, which substantially decreases the required experimental time-frames down to a few days. Furthermore, Tokunaga et al. (Tokunaga et al., 2004) used an X-ray microprobe to characterize uranium concentration profiles, and micro-XANES to determine uranium oxidation state in the solid phase.

4.3.4 Quality Assurance and Control

Due to the sensitivity of diffusion rates to a variety of factors, the following parameters need to be monitored and/or controlled over the course of diffusion experiments (Shackelford, 1991): 1) pH and temperature, as they can influence chemical reactions; and 2) electrical conductivity or a more detailed dissolved ion analysis to monitor potential changes in ionic strength and solution composition, e.g. due to mineral dissolution reactions. Furthermore, mass balance analyses can provide indications of potential, experimental artifacts caused by metal precipitation. Last, blank (control) tests using the same experimental setup but in the absence of the solid phase can determine the maximum solute losses to be expected, e.g. due to metal sorption onto container walls, tubing, etc.

4.4 Summary of Current Knowledge of Uranium Diffusion

As described above, it is understood from both modeling and experimental studies that diffusion processes are influenced by: 1) the electrical charge of the diffusing solute, 2) the degree of compaction and the number of interlayer water molecules in the clay structure, and 3) the electrical double layer structure at the clay/water interface, which is itself impacted by degree of compaction and ionic strength. Below we summarize the current state-of-the-art with respect to uranium(VI) diffusion knowledge and how the charge of U(VI) aqueous species varies with relevant chemical conditions.

4.4.1 Uranium(VI) Aqueous Speciation

There are only a few studies of uranium diffusion into clays and clay-rich geological materials, and even less under well-controlled chemical conditions that allow a clear separation of the three factors described above and their impact on uranium diffusion. With regard to the charge of the diffusing U(VI) species, the influence of relevant chemical conditions on U(VI) aqueous speciation has advanced considerably over the last decade, and it is now recognized that pH and bicarbonate and calcium concentrations each play important roles in determining the predominant aqueous species of U(VI) and its sorption on mineral surfaces (Davis et al., 2004; Fox et al., 2006; Bradbury et al., 2011). To illustrate the complexity of U(VI) aqueous speciation, consider that in a dilute U(VI) solution at pH 7 in the absence of bicarbonate, the predominant U(VI) species is the neutral $UO_2(OH)_2^o$. For the same solution in equilibrium with the partial pressure of CO_2 in air, the predominant species is the anion, $(UO_2)_2CO_3(OH)_3^-$ (in the absence of Ca). However, groundwaters typically are in equilibrium with partial pressures of CO_2 at 1% or greater. At 1% CO_2 at pH 7 in the absence of Ca, the predominant species is the anion, $UO_2(CO_3)_2^{2-}$ (Fig. 4-5). Typical bentonite material that would be used in engineered barriers contains minor amounts of calcite. At 1% CO_2 at pH 7 in equilibrium with calcite, the predominant species is the neutral species, $Ca_2UO_2(CO_3)_3^o$ (Fig. 4-6).

The importance of the neutral species, $Ca_2UO_2(CO_3)_3^o$, in reactive transport modeling of U(VI) transport at contaminated field sites has been recognized for at least 5 years (Curtis et al., 2006; Yabusaki et al., 2008; Ma et al., 2010). However, with regard to nuclear waste disposal in clay-rich environments or within engineered clay barriers, it is only recently been noted that this species may be controlling the sorption of U(VI) and its diffusion in clay-rich environments (Kerisit et al., 2010; Bradbury et al., 2011; Joseph et al., 2011).

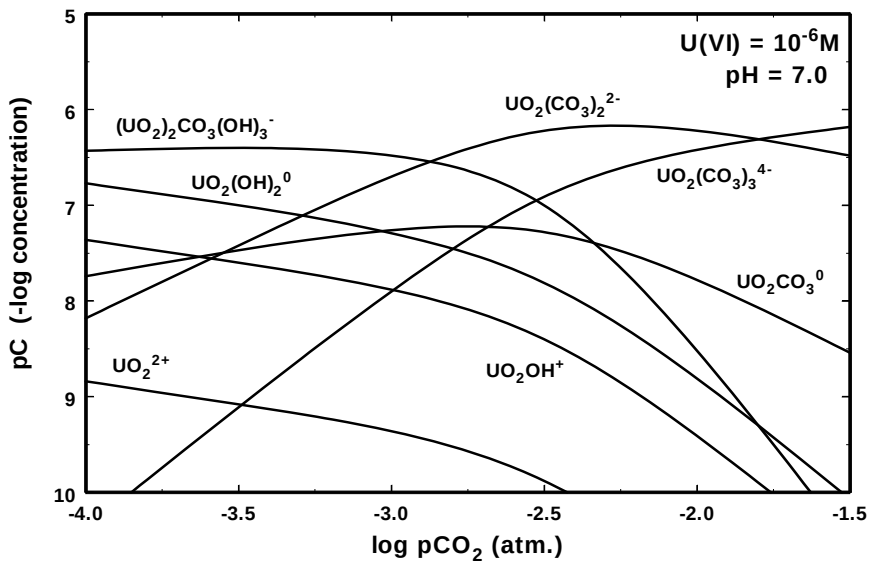

Figure 4-5. Uranium(VI) speciation as a function of the partial pressure of CO_2 in a 1 μM U(VI) solution at pH 7 in the absence of Ca.

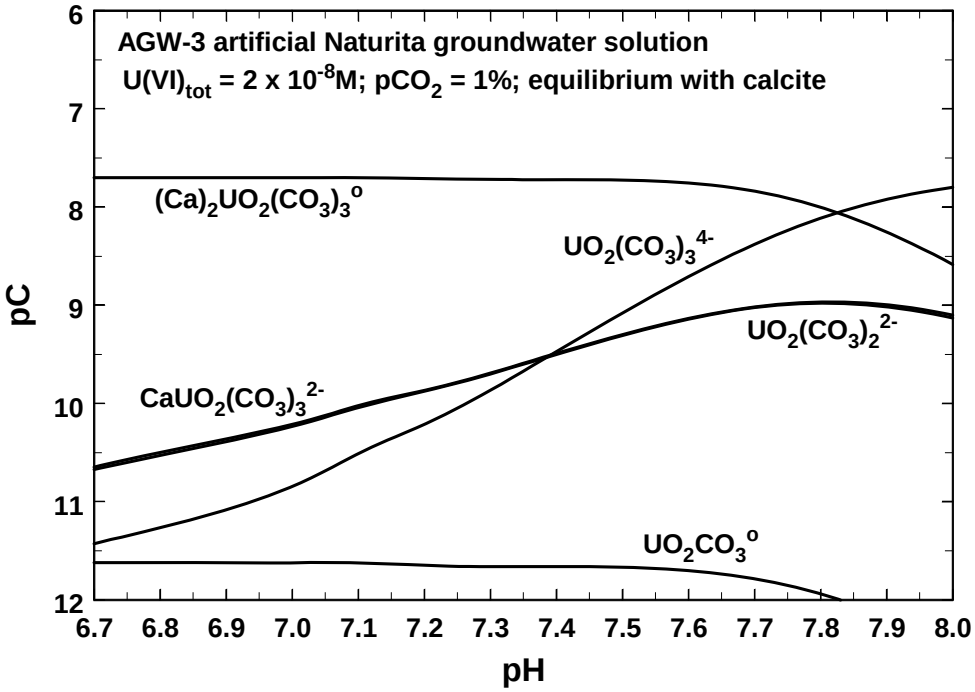

Figure 4-6. Uranium(VI) speciation as a function of pH in a 0.02 μM U(VI) solution in equilibrium with a partial pressure of CO_2 of 1% and in equilibrium with calcite.

Yamaguchi and co-workers (Yamaguchi et al., 1997; Yamaguchi et al., 1998) were among the first to examine the impact of speciation on diffusion of U(VI) under carefully controlled chemical conditions. These authors studied the diffusion of uranium through fractured granite in two different solutions: a) a 0.1M KCl solution at pH 4, in which the presumed predominant species was UO_2^{2+}, and b) a 0.1M $NaHCO_3$ solution at pH 9, with presumed predominant species, $UO_2(CO_3)_3^{4-}$. The observed effective diffusion of U(VI) was four times greater in the latter solution through granite with a total porosity of 0.7%. Although the authors were specifically considering aqueous speciation effects on U(VI) diffusion, the effect of Ca on the experiments is unknown as the concentrations of calcium were not given in the papers.

Maes et al. (Maes et al., 2002) also considered the effects of chemical conditions on uranium diffusion, but only in the broader context of variable redox conditions. The authors determined that under the geochemical conditions prevailing *in situ* in the Boom Clay Formation in Belgium, thermodynamic calculations predicted that the neutral species, $U(OH)_4^o$, should be the predominant uranium species in interstitial water, with its concentration limited by the solubility of uraninite. However, the predicted boundary of the domain with the predominant U(VI) species, $UO_2(CO_3)_3^{4-}$, was very close. The authors conducted an experimental study of U(VI) diffusion within the clay while exposing the system to an electric field to influence the diffusion of cations and anions. The results

indicated that diffusion of U(VI) was probably controlled by a neutral species or cation, lending support to the thermodynamic calculations. However, the influence of dissolved Ca was not considered, as was the case in the Yamaguchi studies (Yamaguchi et al., 1997; Yamaguchi et al., 1998).

4.4.2 Clay-Rich Soils and Sediments

Recent studies of U(VI) diffusion through clay- and silt-rich soils and sediments have considered the impacts of complex aqueous U(VI) speciation more carefully (Tokunaga et al., 2004; Bai et al., 2009; Liu et al., 2010). Tokunaga et al. (Tokunaga et al., 2004) studied the diffusion of U(VI) into two soils (Altamont and Oak Ridge) under variable pH and high uranium concentrations. The high U(VI) concentrations likely caused precipitation of schoepite, $UO_2(OH)_2$ (s), in some of the experiments, making it difficult to fully understand the impacts of aquoues U(VI) speciation on the experiments. Nonetheless, prediction of measured diffusion rates from a model of effective diffusion determined with measured K_d values for U(VI) sorption on the soils was reasonable.

Bai et al. (Bai et al., 2009) measured the effective diffusion of U(VI) through a Hanford silt/clay sample under carefully controlled conditions. Inward-flux diffusion studies were conducted in which U(VI) in both the aqueous and solid phases were measured as a function of distance in the diffusion cell under conditions of constant concentration at the cell boundaries. The effect of sorption kinetics on U(VI) interparticle diffusion was evaluated by comparing sorption-retarded diffusion models with sorption described either as equilibrium or intraparticle diffusion-limited processes. Both experimental and modeling results indicated that: (1) a single pore diffusion coefficient could simulate the diffusion of total aqueous U(VI), and (2) the local equilibrium assumption was appropriate for modeling sorption-retarded diffusion under the given experimental conditions. For the single pore diffusion model, an effective diffusion coefficient for all U(VI) species was estimated as 1.6-1.7 x 10^{-10} m^2/s in an aqueous solution at pH 8.0 and saturated with respect to calcite, as relevant to some subsurface regions of the Hanford site. A tortuosity of 2.45-2.88 was estimated for these experimental system, yielding an apparent diffusivity of total U(VI) of 3.9-4.9 x 10^{-10} m^2/s. The predominant U(VI) species in the solution was $Ca_2UO_2(CO_3)_3^o$, and the measured apparent diffusivity is close to that predicted for the molecular diffusivity of this species in water (Kerisit et al., 2010).

Liu et al. (Liu et al., 2010) investigated U(VI) diffusion through a fine-grained saprolite sediment from Oak Ridge. U(VI) diffusion was studied in a diffusion cell with one cell end in contact with a large, air-equilibrated electrolyte reservoir. The pH, carbonate and U(VI) concentrations in the reservoir solution were varied to investigate the effect of solution chemical composition and uranyl speciation on U(VI) diffusion in 0.05M $NaNO_3$ solutions.

The rates of U(VI) diffusion were evaluated by monitoring the U(VI) concentration in the reservoir solution as a function of time; and by measuring the total concentration of U(VI) extracted from the sediment as a function of time and distance in the diffusion cells. The estimated apparent rate of U(VI) diffusion varied significantly with pH, with the slowest rate observed at pH 7 as a result of strong adsorptive retardation. The estimated retardation factor was generally consistent with a surface complexation model. Numerical simulations indicated that a species-based diffusion model that incorporated both aqueous and surface complexation reactions was required to describe U(VI) diffusion in the low permeability material under variable geochemical conditions. Dissolution or desorption of Ca from the saprolite was not considered in this study because the sediment was washed three times with $NaNO_3$ solution before the experiments, although no data were reported for Ca concentrations after the washing procedure.

4.4.3 Claystone Formations

Other groups have investigated uranium transport in clay-rich rock formations over longer time scales. In particular, the Opalinus Clay formation in Switzerland is a potential host rock for a deep underground nuclear waste repository, and has been studied extensively in laboratory and field investigations. Pekala et al. (Pekala et al., 2009) studied the distribution of U-238, U-234, and Th-230 isotopes in rock samples of the Opalinus Clay from an exploratory borehole. The objective was to assess the extent of long-term migration of U-234 in the rock. The Opalinus Clay has very low hydraulic conductivity and pore water with reduced redox status, and as a result it is expected that U-238 and Th-230 are essentially immobile due to solubility controls. Assuming that U is heterogeneously distributed in the rock, gradients in the supply of U-234 from the rock matrix to the pore water by alpha recoil will be established. In this manner, diffusive redistribution can separate U-234 from its immobile parent U-238, resulting in bulk rock 234U/238U activity disequilibria. This can then provide a means of estimating the mobility of U-234 in the rock if the diffusion rate of 234U is significant compared to its decay rate. The authors carried out sampling on two scales. Cm-spaced samples were collected to study mobility over short distances and homogenized 25 cm segments of a 2 m core section were prepared to provide information on transport over a longer distance. Variations in U and Th content on the cm-scale between clays and carbonate-sandy layers showed that the clay was richer in both elements. The main U-rich phase and U reservoir in the rock was found to micron-sized zircon grains, which had a high U/Th ratio and U-234/U-238 activity ratios below unity. The zircon grains act as constant rate suppliers of U-234 into the rock matrix and the pore water. Some cm-spaced samples showed bulk rock U-234/U-238 activity ratios that were markedly out of equilibrium. In most of them a striking negative correlation between total U content and bulk rock U-234/U-238 activity ratios was observed. This indicated that net U-234 moved from regions of higher supply of U-234 towards those of lower supply, which generally meant transfer from clayey towards

carbonate/sandy portions of the rock. In contrast, the 25 cm samples all had bulk rock U-234/U-238 activity ratios in equilibrium, indicating U immobility in the last 1–1.5 million years on this spatial scale. It was concluded that the small-scale lithological variations which govern U spatial distribution in the Opalinus Clay are the major factor determining U-234 in situ supply rates, regulating its diffusive fluxes and controlling the observed bulk rock U-234/U-238 activity ratios.

In a follow-on study, Pekala et al. (Pekala et al., 2010) studied the Opalinus Clay near its contact with an overlying oxidising aquifer. These data suggested a limited redistribution of U in some of the samples. Observed centimetre-scale U mobility was explained by slow diffusive transport of U-234 in the pore waters of the Opalinus Clay, driven by spatially variable supply by alpha recoil of U-234 from the rock matrix. However, metre-scale mobility was interpreted as a result of infiltration of meteoric water into the overlying aquifer which developed gradients of U concentration across the two rock formations. This triggered a slow in-diffusion of U with U-234/U-238 >1 into the Opalinus Clay.

4.4.4 Bentonite

Studies of uranium diffusion into bentonite clay (compacted or uncompacted) are few in number, especially under well-controlled chemical conditions. Perhaps the best study to date has been by Korichi et al. (Korichi et al., 2010), who investigated the effect of bentonite compaction on the diffusion behavior of uranium. The authors concluded that the dry density of the compacted clay and the aqueous solution properties (pH and ionic strength of background electrolyte) both played important roles in uranium transport through compacted clays. Garcia-Gutierrez et al. (Garcia-Gutierrez et al., 2003) carried out through-diffusion experiments for uranium through FEBEX bentonite compacted to 1.65 kg/dm^{-3} and estimated both effective and apparent diffusion coefficients from the same experiment using different theoretical approaches. However, chemical conditions and U(VI) aqueous speciation were not a component of this study. Muurinen (Muurinen, 1990) also studied uranium diffusion through compacted bentonite MX-80, but chemical conditions were not carefully monitored.

4.5 Research Needs and Plans

As mentioned above, it is understood from both modeling and experimental studies that diffusion processes are influenced by: 1) the electrical charge of the diffusing solute, 2) the degree of compaction and the number of interlayer water molecules in the clay structure, and 3) the electrical double layer structure at the clay/water interface.

Bourg and Sposito (Bourg et al., 2010) have described the manner in which continuum-scale diffusive properties of smectite-rich porous media arise from their molecular- and

pore-scale features. The continuum-scale apparent diffusion coefficients for water tracers and cations decomposes into a sum of pore-scale terms describing diffusion in macropore and interlayer compartments. In bentonite compacted for an engineered barrier surrounding nuclear waste, the smectites will primarily be present in the one- and two-layer hydrate form (i.e., one to two statistical monolayers of water in each smectite interlayer). Under these conditions, anions do not enter the interlayer and can only diffuse through the macropore environments, whereas neutral and cationic solutes can, in principle, diffuse through the clay interlayers.

Zaidan et al. (Zaidan et al., 2003) performed Monte Carlo and molecular dynamics simulations to investigate the interlayer structure of a uranyl-substituted smectite clay. They used a model for dioctahedral montmorillonite with negative charge sites in the octahedral sheet only. Their simulation results for a two-layer hydrate of uranyl-montmorillonite resulted in uranyl cations oriented nearly parallel to the surface normal in an outer-sphere complex. The first coordination shell consisted of five water molecules with an average U-O distance of 2.45 Angstrom, in good agreement with experimental data. Their molecular dynamics results concluded that $UO_2(H_2O)_5^{2+}$ complexes translate within the clay pore through a jump diffusion process, and that first-shell water molecules are exchangeable and interchangeable.

We can see from the above how the U(VI) aqueous speciation may affect U(VI) diffusion rates, as the predominant U(VI) species may be either neutral or anionic species depending on chemical conditions. The anionic U(VI) species may not enter the interlayer when bentonite is compacted. Perhaps even the neutral $Ca_2UO_2(CO_3)_3^o$ will not be able to enter the interlayer because of steric hindrance, as its size is of the order of 1 nm and the 2-layer hydrate interlayer is of the order of 1.4 nm. Thus, U(VI) diffusion into compacted bentonite may be controlled by the supply of cationic U(VI) species, whose concentrations may be orders of magnitude below those of the other species but will vary such that their concentrations can be predicted (at equilibrium) from the pH, bicarbonate, and calcium concentrations.

Diffusion through bentonite with three-layer hydrate smectite particles (i.e., with zero or minor degrees of compaction) might be expected to behave quite differently, as anionic or larger neutral species may be able to enter the interlayer. Furthermore, the influence of electrical double layers and background ionic strength might be expected to play greater roles. In addition, the behavior of bentonites that are initially saturated with the Na^+ ion would be expected to behave quite differently from those initially saturated with Ca^{2+}.

4.5.1 Research Plans

We will perform lab-scale uranium diffusion experiments with compacted bentonite:

1) Under a variety of chemical solution conditions (e.g., pH, salt composition, ionic strength, total carbonate concentration, etc.) and degrees of compaction, to characterize the effects of chemical solution speciation on apparent uranium diffusion rates and its dependence on compaction.

2) With varied experimental temperatures and total uranium concentrations, with a goal to determine activation energies and to distinguish between various (diffusion) processes consistent with a model-based data interpretation.

3) Employ X-ray spectroscopic and electron-based imaging techniques to evaluate diffusion on scales of microns up to one mm.

4) Engage in modeling collaborations with Carl Steefel and Ian Bourg (LBNL) to develop a diffusion model for U(VI) that is consistent with our experimental data.

5. SUMMARY

The EBS and near-field NBS are involved in complex thermal, hydrogeological, mechanical, and chemical processes, such as heat release due to radionuclide decay, multiphase flow (including gas release due to canister corrosion), swelling of buffer materials, radionuclide diffusive transport, waste dissolution and chemical reactions. All these processes are related to each other. An in-depth understanding of these coupled processes is critical for the performance assessment (PA) for EBS, NBS and the entire repository. This report documents the progress to investigate these processes and their coupling, including development of a fully coupled THCM modeling capability, discrete fracture modeling for disturbed-rock zone of a clay repository, and experimental study of uranium diffusion in clay-rich environments and bentonite.

Modeling coupled THMC processes with TOUGHREACT-FLAC

We presented the status of development of coupled THMC model using TOUGHREACT-FLAC that has been linked to provide the necessary numerical framework for the fully coupled THMC modeling. The TOUGHREACT-FLAC simulation approach has been demonstrated and tested for modeling bentonite swelling as a result of changes in saturation and pore-water composition using a simple linear elastic swelling model. An approach for more rigorous swelling modeling has been identified; it is based on linking diffuse double layer (DDL) theory for swelling to a geomechanical double structure model involving micro and macro structural changes. Proposed future work includes extension of the existing implementation of the Barcelona Basic Model (BBM) to the double structure behavior equivalent to the Barcelona Expansive Model (BExM), development of the necessary links between DDL and BExM models for rigorous (mechanistic) modeling of the swelling phenomena, and testing and demonstration of the new model capability with published experimental data.

Discrete fracture modeling for disturbed-rock zone of a clay repository

Repository excavations lead to fracturing in a disturbed rock zone (DRZ) close to the excavations. Extension fractures are formed normal to the minimum principle stress and are sub-parallel to the tunnel side-walls and bedding plane fractures within the buckling zones are oriented mainly by the geometry of the depositional beds. There are also indications that other natural structures, such as tectonic shear zones, impact the resulting fracture patterns in the DRZ. The limited fracturing and effects of fracture self-sealing on fracture connectivity mean that the flow behavior through the DRZ fractures may not be well represented by continuum models. Investigations into discrete fracture models for the DRZ found that only one such model has been constructed. Representing discrete fractures for flow and transport modeling is a challenging problem. Methods to create suitable numerical grids for discrete fractures in a rock matrix for three-dimensional problems such as the DRZ are not easily extended from methods developed for two-dimensional systems. Voronoi gridding methods, which are suitable for integrated finite difference methods, have had considerably less development and use for constructing general three-dimensional polyhedral grids. Voronoi gridding methods for unstructured grids have been developed for two-dimensional systems including systems with discrete fractures and rock matrix. However, ways to represent fractures and fracture intersections for three-dimensional Voronoi grids require further development. Because the DRZ represents a restricted volume domain with particular fracturing patterns, a more direct approach for modeling flow through discrete fractures in the DRZ may be feasible than for the general problem of flow through discrete fracture networks. Items that need to be further investigated include the use of constraints for fracture network geometry, the use of full or reduced-dimensional representations of fractures, and Voronoi gridding methods in three dimensions.

Experimental Study of Uranium Diffusion in Clay-Rich Environments and Bentonite

The primary goal of this study is to characterize the effects of uranium(VI) solution speciation on apparent uranium diffusion rates in clay-rich environments and bentonite. For reactive solutes, such as uranium(VI), apparent diffusion coefficients typically include effects of molecular diffusion processes as well as interactions with the solid phase, such as metal sorption reactions and tortuosity. Recently, it has become more and more evident that apparent diffusion rates can be affected by metal solution speciation and chemical solution conditions, such as pH and aqueous carbonate concentrations. Specifically for clays, it is understood from both modeling and experimental studies that diffusion processes are influenced by: 1) the electrical charge of the diffusing solute, 2) the degree of compaction and the number of interlayer water molecules in the clay structure, and 3) the electrical double layer structure at the clay/water interface. We are developing a systematic, experimental approach to evaluate the effects of chemical solution conditions on apparent uranium diffusion rates, which will aid to improve the predictive capabilities of diffusion-based transport models, and deepen our conceptual understanding of diffusion mechanisms. In this report, we provide: 1) a detailed discussion of potential influences of chemical solution speciation on diffusion coefficients; 2) an overview of current,

experimental diffusion methods; and 3) a critical review of previous uranium diffusion studies. We also briefly summarize current research needs and specific plans for this study.

Integration with Other Work Packages

Research and development activities in this work package are being closely integrated with related activities in other work packages in which LBNL has been involved. For example, the development of the coupled THMC simulator (TOUGHREACT-FLAC3D) has been coordinated with the THC modeling activity in the NBS work package and the THM modeling activity in the EBS work package, and will be emerged into NBS work package in FY12. The experimental study of diffusion in EBS buffer (bentonite) is closely integrated with reactive diffusive transport modeling in the EBS work package, and will be emerged into that work package in FY12.

REFERENCES

Alonso E.E., J. Vaunat, and A. Gens. 1999. Modeling the mechanical behvaviour of expansive clay. Engineering Geology 54: 173-183.

Alonso, U., T. Missana, M. Garcia-Gutierrez, A. Patelli, J. Ravagnan and V. Rigato 2003. Study of the uranium heterogeneous diffusion through crystalline rocks and effects of the "clay-mediated" transport. Scientific Basis for Nuclear Waste Management XXVII, Kalmar, Sweden, Materials Research Society.

Alonso, U., T. Missana, A. Patelli, J. Ravagnan and V. Rigato 2003. RBS and mu PIXE analysis of uranium diffusion from bentonite to the rock matrix in a deep geological waste repository. Nuclear Instruments & Methods in Physics Research Section B-Beam Interactions with Materials and Atoms 207 (2): 195-204.

Alonso E.E., J. Alcoverro, et al (26 co-authors) 2005. The FEBEX Bechmark test. Case Definition and comparison of modelling approaches. Int. J. Rock Mech. & Min. Sci, 42: 611-638.

Alonso, U., T. Missana, M. Garcia-Gutierrez, A. Patelli, M. Siitari-Kauppi and V. Rigato 2009. Diffusion coefficient measurements in consolidated clay by RBS micro-scale profiling. Applied Clay Science 43 (3-4): 477-484.

Appelo, C. A. J., A. Vinsot, S. Mettler and S. Wechner 2008. Obtaining the porewater composition of a clay rock by modeling the in- and out-diffusion of anions and cations from an in-situ experiment. Journal of Contaminant Hydrology 101 (1-4): 67-76.

Bai, J., C. X. Liu and W. P. Ball 2009. Study of Sorption-Retarded U(VI) Diffusion in Hanford Silt/Clay Material. Environmental Science & Technology 43 (20): 7706-7711.

Barraclough, D. and P. H. Nye 1979. Effect of molecular-size in diffusion characteristics in soil. Journal of Soil Science 30 (1): 29-42.

Birkholzer J 2011. *Disposal R&D in Used Fuel Disposition Campaign: A Discussion of Opportunities for Active International Collaborations* (FCR&D-USED-2011-000225), U.S. DOE Used Fuel Disposition Campaign.

Bolt, G. H. 1956. Physico-chemical analysis of the compressibility of pure clays. Géotechnique 6(2): 86–93.

Bond, D. L., J. A. Davis and J. M. Zachara 2008. Uranium(VI) release from contaminated vadose zone sediments: estimation of potential contributions from dissolution and desorption. Developments in earth & environmental sciences, 7. M. O. Barnett and D. B. Kent, Elsevier.

Bourg, I. C., A. C. M. Bourg and G. Sposito 2003. Modeling diffusion and adsorption in compacted bentonite: a critical review. Journal of Contaminant Hydrology 61 (1-4): 293-302.

Bourg, I. C. and G. Sposito 2010. Connecting the Molecular Scale to the Continuum Scale for Diffusion Processes in Smectite-Rich Porous Media. Environmental Science & Technology 44 (6): 2085-2091.

Bourg, I. C., G. Sposito and A. C. M. Bourg 2006. Tracer diffusion in compacted, water-saturated bentonite. Clays and Clay Minerals 54 (3): 363-374.

Bourg, I. C., G. Sposito and A. C. M. Bourg 2007. Modeling cation diffusion in compacted water-saturated sodium bentonite at low ionic strength. Environmental Science & Technology 41 (23): 8118-8122.

Bradbury, M. H. and B. Baeyens 2011. Predictive sorption modelling of Ni(II), Co(II), Eu(IIII), Th(IV) and U(VI) on MX-80 bentonite and Opalinus Clay: A "bottom-up" approach. Applied Clay Science 52 (1-2): 27-33.

Brown, P. L., A. Haworth, S. M. Sharland and C. J. Tweed 1991. Modeling studies of the sorption of radionuclides in the far field of a nuclear waste repository. Radiochimica Acta 52-3: 439-443.

BSC 2004. *Development of Numerical Grids for UZ Flow and Transport Modeling.* ANL-NBS-HS-000015 REV 02. Las Vegas, Nevada: Bechtel SAIC Company. ACC: DOC.20040901.0001.

Crooks, V. E. and R. M. Quigley 1984. Saline leachate migration through clay - a comparative laboratory and field investigation. Canadian Geotechnical Journal 21 (2): 349-362.

Curtis, G. P., J. A. Davis and D. L. Naftz 2006. Simulation of reactive transport of uranium(VI) in groundwater with variable chemical conditions. Water Resources Research 42 (4).

Cussler, E. L. 1997. Diffusion, mass transfer in fluid systems. Cambridge, UK, Cambridge University Press.

Davis, J. A., D. E. Meece, M. Kohler and G. P. Curtis 2004. Approaches to surface complexation modeling of uranium(VI) adsorption on aquifer sediments. Geochimica Et Cosmochimica Acta 68 (18): 3621-3641.

ENRESA 2000. *Full-scale engineered barriers experiment for a deep geological repository in crystalline host rock FEBEX Project*, European Commission**:** 403.

Erhel, J., J.-R. De Dreuzy, B. Poirriez. 2009. Flow Simulation in Three-Dimensional Discrete Fracture Networks, Siam Journal on Scientific Computing, Vol. 31, No. 4, pp. 2688–2705.

Eriksen, T. E., M. Jansson and M. Molera 1999. Sorption effects on cation diffusion in compacted bentonite. Engineering Geology 54 (1-2): 231-236.

Evans, S. D. and S. A. Barber 1964. The effect of cation-exchange capacity, clay content, and fixation on rubidium-86 diffusion in soil and kaolinite systems. Soil Science Society of America Proceedings 28 (1): 53-56.

Fernández, A., J. Cuevas and P. Rivas 2001. Pore water chemistry of the FEBEX bentonite. Mat. Res. Soc. Symp. Proc. 663: 573-588.

Fox, P. M., J. A. Davis and J. M. Zachara 2006. The effect of calcium on aqueous uranium(VI) speciation and adsorption to ferrihydrite and quartz. Geochimica Et Cosmochimica Acta 70 (6): 1379-1387.

Garcia-Gutierrez, M., J. L. Cormenzana, T. Missana, M. Mingarro and U. Alonso 2003. Analysis of uranium diffusion coefficients in compacted FEBEX bentonite. Scientific Basis for Nuclear Waste Management XXVII, Kalmar, Sweden, Materials Research Society.

Gens, A, E. Alonso 1992. A framework for the behaviour of unsaturated expansive clays. Can Geotech J 29:1013–1032.

Gens, A., M. Sánchez, D. Sheng 2006. On constitutive modelling of unsaturated soils. Acta Geotechnica, 1, 137–147.

Guillaumont, R., T. Fanghanel, J. Fuger, I. Grenthe, V. Neck, D. A. Palmer and M. H. Rand 2003. Update on the Chemical Thermodynamics of Uranium, Neptunium, Plutonium, Americium and Technetium. Amsterdam, Elsevier.

Guimarães, L., A. Gens and S. Olivella 2007. Coupled Thermo-Hydro-Mechanical and Chemical Analysis of Expansive Clay Subjected to Heating and Hydration. Transport in Porous Media 66(3): 341-372.

Jackson C.P., A.R. Hoch, S. Todman. 2000. Self-consistency of a heterogeneous continuum porous medium representation of a fractured medium, Water Resources Research, Vol. 36, No. 1, Pages 189-202, January 2000.

Johnson, R. L., J. A. Cherry and J. F. Pankow 1989. Diffusive contaminant transport in natural clay - a field example and implications for clay-lined waste-disposal sites. Environmental Science & Technology 23 (3): 340-349.

Joseph, C., K. Schmeide, S. Sachs, V. Brendler, G. Geipel and G. Bernhard 2011. Sorption of uranium(VI) onto Opalinus Clay in the absence and presence of humic acid in Opalinus Clay pore water. Chemical Geology 284 (3-4): 240-250.

Kamei, G., M. S. Mitsui, K. Futakuchi, S. Hashimoto and Y. Sakuramoto 2005. Kinetics of long-term illitization of montmorillonite - a natural analogue of thermal alteration of bentonite in the radioactive waste disposal system. Journal of Physics and Chemistry of Solids 66(2-4): 612-614.

Kemper, W. D., D. E. L. Maasland and L. K. Porter 1964. Mobility of water adjacent to mineral surfaces. Soil Science Society of America Proceedings 28 (2): 164-167.

Kerisit, S. and C. Liu 2009. Molecular Simulations of Water and Ion Diffusion in Nanosized Mineral Fractures. Environmental Science & Technology 43 (3): 777-782.
Kerisit, S. and C. X. Liu 2010. Molecular simulation of the diffusion of uranyl carbonate species in aqueous solution. Geochimica Et Cosmochimica Acta 74 (17): 4937-4952.

Kim, H.-T., T.-W. Suk, S.-H. Park and C.-S. Lee 1993. Diffusivities for ions through compacted Na-bentonite with varying dry bulk density. Waste Management 13 (4): 303-308.

Kolditz, O. 1995. Modelling Flow and Heat Transfer in Fractured Rocks: Conceptual Model of a 3-D Deterministic Fracture Network, Geothermics, Vol. 24, No. 3, pp. 451--470, 1995.

Komine, H. and N. Ogata 1996. Prediction for swelling characteristics of compacted bentonite. Canadian Geotechnical Journal 33: 11-22.

Komine, H. and N. Ogata 2003. New equations for swelling characteristics of bentonite-based buffer materials. Canadian Geotechnical Journal 40: 460-475.

Korichi, S., A. Bensmaili and M. Keddam 2010. Reactive Diffusion of Uranium in Compacted Clay: Evaluation of Diffusion Coefficients by a Kinetic Approach. Defect and Diffusion Forum 297-301: 275-280.

Lanyon, G.W. 2007. EDZ converter, a structured approach to the derivation of effective properties for combined water and gas flow in the EDZ: Part 1 DFN simulations. Nagra Internal Report *NIB 07-10,* Nagra, 2007.

Lanyon, G.W., R. Senger. 2011. A Structured Approach to the Derivation of Effective Properties for CombinedWater and Gas Flow in the EDZ, Transport in Porous Media, DOI 10.1007/s11242-011-9716-y.

Laredj, N., H. Missoum and k. Bendani 2010. Modeling the effect of osmotic potential changes on deformation behavior of swelling clays. Journal of Porous Media 13(8): 743-748.

Leckenby, R.J., L. Lonergan, S.F. Rogers, D.J. Sanderson. 2007. Study of fracture-induced anisotropy from discrete fracture network simulation of well test responses, From: Lonergan, L., R,J.H. Jolly, K. Rawnsley, D.J. Sanderson (eds), Fractured Reservoirs. Geological Society, London, Special Publications, 270, 117-137.

Ledoux, H. 2007. Computing the 3D Voronoi Diagram Robustly: An Easy Explanation, 4th International Symposium on Voronoi Diagrams in Science and Engineering (ISVD 2007), IEEE Computer Society.

Leroy, P., A. Revil and D. Coelho 2006. Diffusion of ionic species in bentonite. Journal of Colloid and Interface Science 296 (1): 248-255.

Liu, C., J. M. Zachara, W. Yantasee, P. D. Majors and J. P. McKinley 2006. Microscopic reactive diffusion of uranium in the contaminated sediments at Hanford, United States. Water Resources Research 42 (12).

Liu, C., L. Zhong and J. M. Zachara 2010. Uranium(VI) diffusion in low-permeability subsurface materials. Radiochimica Acta 98 (9-11): 719-726.

Ma, R., C. Zheng, H. Prommer, J. Greskowiak, C. Liu, J. Zachara and M. Rockhold 2010. A field-scale reactive transport model for U(VI) migration influenced by coupled multirate mass transfer and surface complexation reactions. Water Resources Research 46.

Madsen, F. T. and M. Muller-vonmoss 1985. Swelling pressure calculated from mineralogical properties of a jurassic opalinum shale, switzerland. Clays and Clay Minerals 33(6): 501-509.

Madsen, F. T. 1998. Clay mineralogical investigations related to nuclear waste disposal. Clay Minerals 33 (1): 109-129.

Maes, N., H. Moors, L. Wang, G. Delecaut, P. De Canniere and M. Put 2002. The use of electromigration as a qualitative technique to study the migration behaviour and speciation of uranium in the Boom Clay. Radiochimica Acta 90 (9-11): 741-746.

Matthäi, S.K., H.M. Nick, C. Pain, I. Neuweiler. 2009. Simulation of Solute Transport through Fractured Rock: A Higher-Order Accurate Finite-Element Finite-Volume Method Permitting Large Time Steps, Transport in Porous Media, DOI 10.1007/s11242-009-9440-z.

McKinley, J. P., J. M. Zachara, C. X. Liu, S. C. Heald, B. I. Prenitzer and B. W. Kempshall 2006. Microscale controls on the fate of contaminant uranium in the vadose zone, Hanford Site, Washington. Geochimica Et Cosmochimica Acta 70 (8): 1873-1887.

Mitchell, J. K. and K. Soga 2005. Fundamentals of Soil Behavior, John Wiley & Sons INC. .

Montes-H, G., N. Marty, B. Fritz, A. Clement and N. Michau 2005. Modelling of long-term diffusion-reaction in a bentonite barrier for radioactive waste confinement. Applied Clay Science 30(3-4): 181-198.

Morrow, C.A.; Moore, D.E.; Lockner, D.A. 2000. "The Effect of Mineral Bond Strength and Adsorbed Water on Fault Gouge Frictional Strength", Geophysical Research Letters, Vol. 27, No. 6. Pp. 815-818.

Muurinen, A. 1990. Diffusion of uranium in compacted sodium bentonite. Engineering Geology 28 (3-4): 359-367.

Narasimhan, T.N., P.A. Witherspoon. 1976. An Integrated Finite Difference Method for Analyzing Fluid Flow in Porous Media, Water Resources Research, Vol. 12, No. 1, February 1976.

Nick, H.M., S.K. Matthäi. 2011a. Comparison of Three FE-FV Numerical Schemes for Single- and Two-Phase Flow Simulation of Fractured Porous Media, Transport in Porous Media, DOI 10.1007/s11242-011-9793-y.

Nick, H.M., S.K. Matthäi. 2011b. A Hybrid Finite-Element Finite- Volume Method with Embedded
Discontinuities for Solute Transport in Heterogeneous Media, Vadose Zone J. 10:299–312, doi:10.2136/vzj2010.0015.

Nicollin, F., D. Gibert, N. Lesparre and C. Nussbaum. 2010. Anisotropy of electrical conductivity of the excavation damaged zone in theMont Terri Underground Rock Laboratory, Geophysical Journal International (2010) 181, 303–320.

Nutt M. 2011. *Used Fuel Disposition Campaign Disposal Research and Development Roadmap* (FCR&D-USED-2011-000065 REV0), U.S. DOE Used Fuel Disposition Campaign.

Ochs, M., B. Lothenbach, H. Wanner, H. Sato and M. Yui 2001. An integrated sorption-diffusion model for the calculation of consistent distribution and diffusion coefficients in compacted bentonite. Journal of Contaminant Hydrology 47 (2-4): 283-296.

OECD 2003. *Engineering barrier systems and the safety of deep geological repositories* (State-of-the-art Report), ISBN 92-64-18498-8.
Onikata, M., M. Kondo, N. Hayashi and S. Yamanaka 1999. Complex formation of cation-exchanged montmorillonites with propylene carbonate; osmotic swelling in aqueous electrolyte solutions. Clays and Clay Minerals 47(5): 672-677.

Paluszny, A., S.K. Matthäi, M. Hohmeyer. 2007. Hybrid finite element–finite volume discretization of complex geologic structures and a new simulation workflow demonstrated on fractured rocks, Geofluids (2007) 7, 186–208.

Pekala, M., D. K. A. Jan, H. N. Waber, T. Gimmi and P. Alt-Epping 2009. Transport of U-234 in the Opalinus Clay on centimetre to decimetre scales. Applied Geochemistry 24 (1): 138-152.

Pekala, M., J. D. Kramers and H. N. Waber 2010. $^{234}U/^{238}U$ activity ratio disequilibrium technique for studying uranium mobility in the Opalinus Clay at Mont Terri, Switzerland. Applied Radiation and Isotopes 68 (6): 984-992.

Porter, L. K., W. D. Kemper, R. D. Jackson and B. A. Stewart 1960. Chloride diffusion in soils as influenced by moisture content. Soil Science Society of America Proceedings 24 (6): 460-463.

Pusch, R. 1992. Use of bentonite for isolation of radioactive-waste products. Clay Minerals 27 (3): 353-361.

Pusch, R. 2006. The performance of clay barriers in repositories for high-level radioactive waste. Nuclear Engineering and Technology, 38, August 2006.

Rameback, H., Y. Albinsson, M. Skalberg, U. B. Eklund, L. Kjellberg and L. Werme 2000. Transport and leaching of technetium and uranium from spent UO_2 fuel in compacted bentonite clay. Journal of Nuclear Materials 277 (2-3): 288-294.

Reichenberger, V., H. Jakobs, P. Bastian, R. Helmig. 2006. A mixed-dimensional finite volume method for two-phase flow in fractured porous media, Advances in Water Resources 29 (2006) 1020–1036.

Rowe, R. K., C. J. Caers and F. Barone 1988. Laboratory determination of diffusion and distribution coefficients of contaminants using undisturbed clayey soil. Canadian Geotechnical Journal 25 (1): 108-118.

Rutqvist J., Y. Ijiri and H.Yamamoto 2011. Implementation of the Barcelona Basic Model into TOUGH-FLAC for simulations of the geomechanical behavior of unsaturated soils. Computers & Geosciences, 37, 751-762.

Rutqvist J. and C.-F. Tsang 2008. *Review of SKB's work on coupled THM processes within SR-Can: External review contribution in support of SKI's and SSI's review of SR-Can.* Swedish Nuclear Power Inspectorate (SKI) Technical Report 2008:08.

Sacchi, E., J.-L. Michelot, H. Pitsch, P. Lalieux and J.-F. Aranyossy 2001. Extraction of water and solution from argellaceous rock for geochemical characterisation: Methods, processes, and current understanding. Hydrogeology Journal 9: 17-33.

Sánchez, M., A. Gens, L. do N. Guimarães, S. Olivella 2005. A double structure generalized plasticity model for expansive materials. Int J Numer Anal Meth Geomech, 29, 751–787. 1.

Schanz, T. and S. Tripathy 2009. Swelling pressure of a divalent-rich bentonite: Diffuse double-layer theory revisited. Water Resour. Res. 45: W00C12.

Selim, H. M. and M. C. Amacher 1997. Reactivity and transport of heavy metals in soils. Boca Raton, CRC Press, Inc.

Shackelford, C. D. 1991. Laboratory diffusion testing for waste disposal - a review. Journal of Contaminant Hydrology 7 (3): 177-218.

Shackelford, C. D. and D. E. Daniel 1991. Diffusion in saturated soil. I: Background. Journal of Geotechnical Engineering-Asce 117 (3): 467-484.

Sridharan, A. and M. S. Jayadeva 1982. Double layer theory and compressibility of clays. Geotechnique 32(2): 133-144.

Sukumar, N. 2003. Voronoi cell finite difference method for the diffusion operator on arbitrary unstructured grids, International Journal for Numerical Methods in Engineering, 2003; 57:1–34 (DOI: 10.1002/nme.664).

Syihab, Z. 2009. Simulation of Discrete Fracture Network Using Flexible Voronoi Gridding, Ph.D. Dissertation, Texas A&M University.

Thomas, H. R. and Y. He 1995. Analysis of coupled heat, moisture and air transfer in a deformable unsaturated soil. Gdotechnique 45(4): 677-689.

Thury, M. 2002. The characteristics of the Opalinus Clay investigated in the Mont Terri underground rock laboratory in Switzerland. Comptes Rendus Physique 3(7-8): 923-933.

Tokunaga, T. K., J. M. Wan, J. Pena, S. R. Sutton and M. Newville 2004. Hexavalent uranium diffusion into soils from concentrated acidic and alkaline solutions. Environmental Science & Technology 38 (11): 3056-3062.

Tripathy, S., A. Sridharan and T. Schanz 2004. Swelling pressures of compacted bentonites from diffuse double layer theory. Canadian Geotechnical Journal 41: 437-450.

Tsang, C.F.; Birkholzer, J.; Liu, H.H. 2010. A Review of Key Processes and Outstanding Issues Related to Radioactive Waste Repositories in Clay Formations, DOE Used Fuel Disposition Campaign, Lawrence Berkeley National Laboratory.

van der Putte, T. 2009. Using the discrete 3D Voronoi diagram for the modelling of 3D continuous information in geosciences, Master Thesis, Geographical Information Management and Applications, Utrecht University, Netherlands.

Van Loon, L. R., M. A. Glaus and W. Mueller 2007. Anion exclusion effects in compacted bentonites: Towards a better understanding of anion diffusion. Applied Geochemistry 22 (11): 2536-2552.

van Olphen, H. 1977. An Introduction to Clay Colloid Chemistry: For Clay Technologists, Geologists and Soil Scientists, Wiley-Interscience, New York.

van Schaik, J. C. and W. D. Kemper 1966. Chloride diffusion in clay-water system. Soil Science Society of America Proceedings 30: 22-25.

Villar, M.E.., E. Castellano, D.Romero, A. Lloret 2006. Experimental evidence of the interaction between THM behavior and chemistry in bentonite. In Proceedings of the GEOPROC2006 International symposium: 2nd International Conference on Coupled Thermo-hydro-mechanical-chemical processes in Geosystems and Engineering, HoHai University, Nanjing, China, May 22-25, 2006, p. 380-385 (2006).

Wakim, J., F. Hadj-Hassen and L. De Windt 2009. Effect of aqueous solution chemistry on the swelling and shrinkage of the Tournemire shale. International Journal of Rock Mechanics and Mining Sciences 46(8): 1378-1382.

Wang Y., M. Simpson, S. Painter, H. Liu, A. B. Kersting 2011. Natural system evaluation and tool development – fy11 progress report. FCRD-USED-2011-000223.

Wersin, P. 2003. Geochemical modelling of bentonite porewater in high-level waste repositories. Journal of Contaminant Hydrology 61 (1-4): 405-422.

Xu, T., N. Spycher, E. Sonnenthal, G. Zhang, L. Zheng and K. Pruess 2011. TOUGHREACT Version 2.0: A simulator for subsurface reactive transport under non-isothermal multiphase flow conditions. Computers & Geosciences 37(6): 763-774.

Yabusaki, S. B., Y. Fang and S. R. Waichler 2008. Building conceptual models of field-scale uranium reactive transport in a dynamic vadose zone-aquifer-river system. Water Resources Research 44 (12).

Yamaguchi, T. and S. Nakayama 1998. Diffusivity of U, Pu and Am carbonate complexes in a granite from Inada, Ibaraki, Japan studied by through diffusion. Journal of Contaminant Hydrology 35 (1-3): 55-65.

Yamaguchi, T., Y. Sakamoto, S. Nakayama and T. T. Vandergraaf 1997. Effective diffusivity of the uranyl ion in a granite from Inada, Ibaraki, Japan. Journal of Contaminant Hydrology 26 (1-4): 109-117.

Yong S., P.K.Kaiser, S. Loew, Influence of tectonic shears on tunnel-induced fracturing, International Journal of Rock Mechanics & Mining Sciences 47 (2010) 894–907.

Yoshida, H., M. Monsecour and I. R. Basham 1991. Use of microscopic techniques in migration studies in boom clay. Radiochimica Acta 52-3: 133-138.

Zaidan, O. F., J. A. Greathouse and R. T. Pabalan 2003. Monte Carlo and molecular dynamics simulation of uranyl adsorption on montmorillonite clay. Clays and Clay Minerals 51 (4): 372-381.

Zheng, L., J. Samper and L. Montenegro 2008. Inverse hydrochemical models of aqueous extracts tests. Physics and Chemistry of the Earth, Parts A/B/C 33(14-16): 1009-1018.

Zheng, L., J. Samper, L. Montenegro and A. M. Fernández 2010. A coupled THMC model of a heating and hydration laboratory experiment in unsaturated compacted FEBEX bentonite. Journal of Hydrology 386(1-4): 80-94.

Zhou, J., X. H. Lu, Y. R. Wang and J. Shi 2002. Molecular dynamics study on ionic hydration. Fluid Phase Equilibria 194: 257-270.